

This is to certify that the

thesis entitled

**CONTACT PROBLEMS BETWEEN A RIGID
PUNCH AND A LAYERED ELASTIC SOLID**

presented by

Jianwei Bai

has been accepted towards fulfillment
of the requirements for

M.S. degree in Engineering Mechanics


Major professor

Date August 14, 2002

**CONTACT PROBLEMS BETWEEN A RIGID PUNCH AND A LAYERED ELASTIC
SOLID**

By

Jianwei Bai

A THESIS

**Submitted to
Michigan State University
in partial fulfillment of the requirements
for the degree of**

MASTER OF SCIENCE

Department of Mechanical Engineering

2002

ABSTRACT

CONTACT PROBLEMS BETWEEN A RIGID PUNCH AND A LAYERED ELASTIC SOLID

By

Jianwei Bai

In this work, the generalized plane strain problem of the contact of a rigid punch and a layered elastic solid is reduced to an integral equation by using Fourier Transforms. A numerical scheme involving matrix inversion is used to obtain the approximate solution to the integral equation. The method is general enough to deal with punch problems with various arrangements of layered structures. The problems under consideration are divided into two categories: conforming contact and non-conforming contact, according to the geometry of the rigid punches. Both single-layered and multi-layered structures are studied in each contact setting. The distribution of contact pressure and the relationship between the total load and the indentation depth are obtained for each case. The effects of the layer geometry and the material properties on the responses of the structure are examined in details. The results provide useful guidance in the design and analysis of such structures under localized loadings.

To my beloved ones

ACKNOWLEDGMENTS

There are many individuals who have contributed to my success at finally getting my thesis completed. I will attempt to thank most of them here, but I acknowledge that many more helped.

Firstly, as far as my time at MSU is concerned, I owe a great deal to my advisor, Professor Hungyu Tsai. Over the past two years, he has given me a tremendous amount of encouragement, support, and guidance. It is he who has taught me the detailed work of scientific research and advised me with valuable tips of life. I really appreciate his patience and encouragement when I was suffering. His contribution to my life is indescribable. I wish I will have a chance to pay back all his support and help.

Secondly, I wish to thank my committee members, including Professor Patrick Kwon and Professor Zhengfang Zhou, for all their support. And my thanks also go to Professor Dahsin Liu, who gave me his warmhearted help and guidance.

Many friends deserve my thanks for their help and advice both in study and in life. It is they who make my life in East Lansing enjoyable and comfortable. They include Guojing Li, Xinjian Fan, Xu Ding, Yuwei Chi, Hui Cao, Nan Song, Jun Wu, and all the members of our basketball group.

I am thankful to my parents and sibling for their endless love, support, and teaching me the value of challenge and perseverance. I am indebted to them. I hope I can recompense them in the near future.

Last but not least, I would like to recognize my girlfriend, Lan Hui. I cannot even begin to explain how much love and support she has given me over the years. Even though she is thousands of miles away, I can feel her love and care every second, and I need her every step of the way. I am looking forward to spending the rest of my life “geographically” closer to her.

TABLE OF CONTENTS

| | |
|--|------|
| LIST OF TABLE | vii |
| LIST OF FIGURES..... | viii |
| CHAPTER 1 INTRODUCTION | 1 |
| 1. 1 Introduction and Literature Review | 1 |
| 1. 2 Outline of Present Work..... | 9 |
| CHAPTER 2 FOURIER TRANSFORMS FOR TWO-DIMENSIONAL STRESS SYSTEMS..... | 11 |
| 2. 1 Introduction | 11 |
| 2. 2 Plane Strain | 13 |
| 2. 3 Solution of the Two-dimensional Biharmonic Equation..... | 15 |
| CHAPTER 3 APPLICATION OF FOURIER TRANSFORMS TO DIFFERENT CONTACT PROBLEMS | 20 |
| 3. 1 Formulation of the Contact Problems of the Action of Rigid Punches on an Elastic Solid | 20 |
| 3. 2 Conforming Contact Problem | 25 |
| 3. 2. 1 A Numerical Procedure for Solving Contact Pressure..... | 25 |
| 3. 2. 2 Rigid Flat Punches on a Single-layered Elastic Solid..... | 33 |
| 3. 2. 3 Rigid Flat Punches on a Multi-layered Elastic Solid | 41 |
| 3. 3 Non-conforming Contact Problem | 54 |
| 3. 3. 1 Rigid Cylinders on a Single-layered Elastic Solid..... | 54 |
| 3. 3. 2 Rigid Cylinders on a Multi-layered Elastic Solid | 67 |
| CHAPTER 4 CONCLUSIONS AND FUTURE WORK | 74 |
| 4. 1 Conclusions | 74 |
| 4. 2 Future Work | 76 |
| BIBLIOGRAPHY | 77 |

LIST OF TABLE

| | |
|---|----|
| Table 3.1 Numerical solutions of total loads for different thicknesses and Young's moduli of middle layers | 51 |
|---|----|

LIST OF FIGURES

| | |
|---|----|
| Figure 2.1. Stress components of two-dimensional problems on an element of an elastic body | 12 |
| Figure 3.1 General contact problem..... | 20 |
| Figure 3.2 Conforming contact problem..... | 24 |
| Figure 3.3 Non-conforming contact problem..... | 24 |
| Figure 3.4 The trapezoidal rule | 28 |
| Figure 3.5 The triangular rule | 28 |
| Figure 3.6 The contact problem between a rigid flat punch and a half space..... | 30 |
| Figure 3.7 Comparison between numerical solution and exact solution of contact problem by a rigid flat punch on a half space | 33 |
| Figure 3.8 Rigid flat punches on a single-layered elastic solid..... | 34 |
| Figure 3.9 Contact pressure variations for various thicknesses of the solid | 37 |
| Figure 3.10 Total loads versus thicknesses of the solid..... | 37 |
| Figure 3.11 Total loads versus more thicknesses of the solid..... | 38 |
| Figure 3.12 Contact pressure variations for different indentation depths..... | 38 |
| Figure 3.13 Total load versus indentation..... | 39 |
| Figure 3.14 Rigid punches on a multi-layered elastic solid..... | 41 |
| Figure 3.15 Comparison of contact pressures between non-middle layer and thin middle layer..... | 49 |
| Figure 3.16 Influence of various layer thicknesses on contact pressure | 49 |
| Figure 3.17 Influence of Poisson's ratios on contact pressure..... | 50 |
| Figure 3.18 Effect of Young's moduli of middle layers on contact pressure | 50 |

| | |
|--|----|
| Figure 3.19 Total loads versus middle layer thicknesses | 51 |
| Figure 3.20 Rigid cylinders on a single-layered elastic solid | 55 |
| Figure 3.21 Comparison between numerical solution and exact solution of contact problem by a rigid cylinder on a half space | 60 |
| Figure 3.22 Comparison of results between 40 points and 50 points | 60 |
| Figure 3.23 Contact pressure distribution for various a/b , $R/a=10$ | 62 |
| Figure 3.24 Contact pressure distribution for various a/b , $R/a=2$ | 62 |
| Figure 3.25 Contact pressure distribution for various R/a , $a/b=0.1$ | 63 |
| Figure 3.26 Contact pressure distribution for various R/a , $a/b=1$ | 63 |
| Figure 3.27 Total loads versus half contact lengths | 64 |
| Figure 3.28 Relationship between half contact length and indentation depth | 64 |
| Figure 3.29 Total loads versus indentation depths | 65 |
| Figure 3.30 Normal displacements in the contact area | 65 |
| Figure 3.31 Rigid cylinders on a multi-layered elastic solid..... | 67 |
| Figure 3.32 Layer thickness' effect on contact pressure distribution | 70 |
| Figure 3.33 Poisson's ratio's effect on contact pressure distribution | 70 |
| Figure 3.34 Young's modulus' effect on contact pressure distribution | 71 |
| Figure 3.35 Contact pressure variations for various half contact lengths | 71 |
| Figure 3.36 Total loads for different half contact lengths..... | 72 |
| Figure 3.37 Half contact lengths versus indentation depths..... | 72 |

Chapter 1

INTRODUCTION

1. 1 Introduction and Literature Review

Most mechanical systems consist of components that are in contact with each other. Hence the study of contact mechanics find its application in almost every corner of solid mechanics, although it has often been limited to mechanisms whose very purpose is to realize a sliding or a rolling contact. Classical applications include devices such as bolts, joints, hinges and roller bearings, and manufacturing processes such as material forming, drawing, molding and machining, as they occur in traditional practice of mechanical engineering. More recent and ambitious applications extend to crash simulations, projectile impacts, fluid-solid interactions, plate tectonics and human joints, as engineering analysis is performed in safety engineering, geology and bioengineering.

As mentioned above, in almost every structural and mechanical system, there exists the situation in which one body comes in contact with another. It is obvious, therefore, that the character of the contact plays a fundamental role in the behavior of the structure: its deformation, its motion, the distribution of stresses, etc.

Despite the fundamental role of contact in the mechanics of solids and structures, contact effects are rarely taken into account in structural analysis. The reason is that the modeling of contact phenomena poses serious difficulties—conceptual, mathematical, and

computational—which are far more complex than those encountered in classical linear structural mechanics. When two bodies are brought into contact, the actual contact surface and the traction distribution over the contact surface are unknown. The boundary conditions on this unknown surface often involve complicated relations between the displacements and the stresses of the bodies to reflect the surface properties of the contact area. As a result, mathematical analysis of contact and the description of the motion of the bodies in contact become extremely complicated.

The study of contact problems in elasticity began in the nineteenth century. In 1882, Hertz [1] successfully treated a static contact problem in elasticity. He considered the equilibrium of two elastic bodies in contact on surfaces whose projection in the plane were conic sections, and he obtained formulas for the contact pressure and indentation under the assumption that the contact area was elliptical. The results of Hertz can be applied to several special problems, e.g., the contact of a circular cylinder or a sphere with a rigid foundation, half-cylinders on foundations, etc. Such problems are referred to as Hertz-type or Hertzian contact problems.

Later Love [2] studied pressure between two bodies in contact in his work, and solutions about this problem were given. In the meantime, the Hertz's theory of impact was summarized. Johnson [3] also did an informative review. In his work, the existence of a solution for the problem of finding the stresses and the displacements in an elasto-plastic body in frictionless contact with a rigid body was proved. Finite element methods for some special cases were also presented.

Several important contributions to the study of contact problems in elasticity were made by the Russian school of elasticians during the first half of the twentieth century. The integral equation methods were developed by Galin [4] in his pioneering book on contact problems. Muskhelishvili's treatise [5] was the basis for much of the Russian work, particularly that using complex variable methods. He developed the methods of complex potentials and conformal maps, and applied them into solving contact problems. Lure [6] gave the outline of the development of the work on contact problems up to the 1950's. The solution for the three-dimensional contact problems between rigid punch and half-space elastic body was also presented in the work.

Much of the Russian work on contact problems is concerned with rigid punch problems (or "rigid stamp" problems, as some refer to them) in which a rigid frictionless body (the punch) is indented into an elastic medium. Typically, the geometry and loading in the classical punch problems are simple and ideal and the contact surface is assumed to be known in advance. These situations are particularly well suited for analysis by classical methods such as those employing the theory of linear integral equations, complex potentials and conformal maps, etc.

A typical situation is, for example, the problem of a homogeneous, isotropic, elastic half-space $\bar{\Omega} = \{(x_1, x_2, x_3) \in \mathfrak{R}^3 | x_3 \geq 0\}$ (x_i being the Cartesian coordinates) indented along the x_3 -axis by the amount α by a rigid punch, the contour of which is defined by

$$x_3 = \rho(x_1, x_2), \quad \rho(0,0) = 0. \quad (1)$$

If P is the total external force applied on the punch parallel to the x_3 -axis, then the contact pressure $\sigma = \sigma(x_1, x_2)$ will satisfy the system of equations

$$\frac{1-\nu^2}{\pi E} \int_{\Gamma_c} \frac{\sigma(\xi_1, \xi_2) d\xi_1 d\xi_2}{\left[(x_1 - \xi_1)^2 + (x_2 - \xi_2)^2 \right]^{\frac{3}{2}}} = \alpha + \rho(x_1, x_2) \quad (2)$$

$$\int_{\Gamma_c} \sigma(\xi_1, \xi_2) d\xi_1 d\xi_2 = P \quad (3)$$

$$\sigma|_{\partial\Gamma_c} = 0 \quad (4)$$

Where ν is the Poisson's ratio, E is the Young's modulus for the half-space, and $\Gamma_c \subset \overline{\Omega}$ is the contact surface. Equation (2) is merely an application of Boussinesq's solution for the displacement of an elastic half-space due to a normal unit point load at point $(\xi_1, \xi_2, 0)$; (3) is a global equilibrium condition. In addition, we must have

$$\begin{aligned} \sigma(x_1, x_2) &\geq 0 && \text{in } \Gamma_c \\ \sigma(x_1, x_2) &= 0 && \text{in } g - \Gamma_c \end{aligned} \quad (5)$$

Where $g = \{(x_1, x_2, x_3) \in \mathcal{R}^3 | x_3 = 0\}$. When Γ_c is known, equations (2) and (3) constitute a system of linear integral equations which can be solved for $\sigma = \sigma(x_1, x_2)$ and α . A number of closed-form solutions are known for such cases. If Γ_c is not known in advance, the problem is nonlinear and another condition, such as the "free boundary condition" (4) must be included in analysis. Nevertheless, exact solutions for some very special cases are known. An excellent treatise on the analysis of contact problems by classical methods has been written by Gladwell [7]. This work also contains many additional references to papers on this subject.

Problems concerning the contact between elastic bodies have provided a challenge to applied mathematicians ever since the work of Hertz in the 1880's. A powerful mathematical tool which has been sharpened by its use in elasticity theory is the integral transforms. Integral transforms were developed during the nineteenth century, however, it was the work of I. N. Sneddon in "Fourier Transforms" (1951) [8] that showed how they could be used for the actual solutions of the difficult boundary value problems of elasticity theory. In particular he reworded dual integral equations to make them accessible to applied mathematicians. Through his writings, his influence can be traced in much of the modern research on classical contact problems.

In recent years, layered solids are widely used in highly technological applications. The contact problem of layered solids has been of considerable interest in various fields of science and engineering, especially in aircraft and spacecraft structures. Layered solids are also used in situations where there is a need for the surface properties to be different from those of the bulk material. In bearing surfaces coated with a thin layer the contact stresses can be substantially non-Hertzian depending on the elastic properties of the layer and the base material ([9], [10], [14] and [15]). Therefore, a generalized plane strain analysis of contact of layered elastic solids will be essential in analyzing, for example, roller bearings where the rollers, races or both have surface layers of different elastic properties.

A number of solutions to the problem of an elastic layer on a rigid substrate have been presented in the literature. In the 1950's, Hannah [9] first considered a plane stress

problem for a thin elastic layer over a rigid substrate. The problem was formulated in terms of an integral equation. A conclusion from photoelasticity was utilized to obtain a solution for the stress function, which was appropriate to an isolated force on a free surface of a thin elastic layer over a rigid infinite substrate. Influences of elastic modulus and layer thickness on contact length and contact pressure about fixed and slipped inner boundary conditions were presented.

Aleksandrov [10] [11] obtained an approximate solution for a plane strain problem of the contact between a die and an elastic layer on a rigid substrate. Numerical results for a kernel of integral equation were presented, where the kernel was assumed to be represented as a power series, and solutions were obtained for small values of the ratio of half contact length, a , to the layer thickness, h . Later Aleksandrov [12] [13] introduced the asymptotic methods and their application in both the solutions of plane and three-dimensional contact problems. He had also obtained asymptotic solutions for both small and large values of a/h .

Based on the work of Hannah and Aleksandrov, Miller [14] developed a truncated cosine series solution to an integral equation for the pressure distribution about the indentation of a thin elastic layer by a smooth rigid cylinder. Tables of results were given which allowed the calculation of pressure distribution when the contact length was less than four times the layer thickness.

Further, Meijers [15] got asymptotic solutions for large and small values of a/h for a rigid cylinder indenting on an elastic layer connected rigidly to a rigid foundation. It was assumed that there was no friction between the cylinder and the layer and that the cylinder was long enough to ensure a plane deformation. Meijers' approximate solution was based on the truncation of series expression for the kernel function. He also showed that numerical solutions could be obtained for any arbitrary value of a/h and the Poisson's ratio varying in the range $0 \leq \nu \leq 0.5$.

Tu [16] considered the axially symmetric contact problem of a plate pressed between two identical spheres. The integral equation for the unknown contact stress distribution was approximated by a set of linear algebraic equations whose solution yielded the unknown pressure values of the approximate distribution. The contact radius and the maximum contact stress were then computed numerically from this solution and were presented in terms of the total load, the radius of the sphere, and the plate thickness.

Wu and Chiu [17] presented a mathematical formulation of a plane-strain problem of an elastic layer supported on a half-space foundation and indented by a cylinder. And later Pao, Wu, and Chiu [18] reported some numerical results of their analysis. They considered two special cases about the layer-foundation interface, one with the indented layer in frictionless contact with the half space and the other with the indented layer perfectly bonded to the half space.

Abblas and Kuipers [19] [20] [21] also did some work about the two dimensional contact problems of the cylindrical stamp or the rectangular block pressed into a thin or thick elastic layers. An asymptotic solution was found for the contact problems. Two cases were considered: a layer that was fixed to a rigid base and a layer that could slide without friction along the base. Compressible and incompressible materials were both treated.

In 1970's, Gladwell [22] considered some plane, frictionless, and unbonded contact problems. The integral equation relating the unknown contact pressure to the specified displacement in the contact region was solved approximately by using an expansion in terms of Chebyshev polynomials. Examples were given, and graphs of results were also presented.

Recently, Scalia [23] [24] solved a static problem about a contact of the rigid punch above a linear porous elastic strip based on a rigid half-plane without friction. He developed an analytical approach to the static contact problem in which the problem was reduced to an integral equation with a convolution kernel. Then he applied a co-location technique to solve this equation. Finally he studied the distribution of the contact pressure for particular values of physical and geometrical parameters.

Wozniak, and Hummel et al. [25] studied some axisymmetric contact problems for an elastic layer pressed by a rigid sphere or by a rigid flat cylinder. The layer was assumed to rest on the rigid half space with a near-boundary cylindrical excavation that was filled with a deformable material. The Hankel integral transforms were applied and the

problems were reduced to systems of integral equations. The numerical analysis was performed to display the effects of geometrical parameters and elastic modulus on the distribution of the contact pressure.

All the work presented so far demonstrated that contact problems of rigid punches on a half space or an elastic layer were abundantly studied. However, not as much analytical work has been performed on contact problems of rigid punches pressing on a multi-layered elastic solid. Obviously, research needs to be done in this area.

1. 2 Outline of Present Work

In the work, the generalized plane strain problem of the contact of rigid punches and a layered elastic solid is reduced to an integral equation by using Fourier Transforms. A numerical procedure is introduced to solve the contact pressure. Numerical solutions are obtained by replacing the integral equation by a matrix inversion. To testify the numerical procedure, first we consider a static contact problem of rigid punches indenting on an infinite elastic solid, because for this case, we can obtain exact analytical solutions. Comparisons of the numerical results with exact analytical solutions of the half-space contact problems are made. And the confirmation of validity and feasibility of the numerical solution procedure is performed.

The contact problems are divided into two cases: conforming contact problem and non-conforming contact problem, according to the different rigid punches. By utilizing the

numerical solution procedure, the solutions for the static contact problem of a finite single-layered medium are obtained. The distribution of contact pressures, the relationships between total loads and indentation depths are illustrated in diagrams.

Further, the method is extended to the static problem about the contact of the rigid punches on a multi-layered solid. Results for determining the actual contact pressure in the contact zone and the relationship between contact pressure and size of contact zone for a wide range of layer thicknesses are presented for practical cases. The relationships between total loads and indentation depths, total loads and half contact lengths, half contact lengths and indentation depths are plotted graphically. Meanwhile, the effects of physical and geometrical properties of middle layers on the distribution of the contact pressure are also presented.

Chapter 2

FOURIER TRANSFORMS FOR TWO-DIMENSIONAL STRESS SYSTEMS

2. 1 Introduction

Integral transform is a very useful and powerful mathematical tool in elasticity theory. Its use in the analysis of contact problems is presented by Sneddon [8].

Usually the problems that we meet are three-dimensional. For simplicity, many cases can be treated as two-dimensional problems. The two-dimensional problems solved can, of course, be subjected to experimental verification only in an imperfect fashion. But their solutions provide us with a sufficiently good picture of the distribution of stress set up in the corresponding three-dimensional case to be of use in the design of structures. There are lots of contact problems that can be treated as two-dimensional problems. The following is how the solution of these two-dimensional contact problems may be obtained by the use of the theory of Fourier Transforms.

There are two main kinds of two-dimensional problems in elasticity: plane strain and plane stress [26]. It is found that, when a body whose dimension in the z direction is very large is loaded by forces that are perpendicular to the longitudinal elements and do not vary along the length, it may be assumed that all cross sections are in the same condition.

Normal sections of the body remain plane and the body retains its original form. There is no axial displacement at every cross section. Any distortion possessing these characteristics is termed plane strain.

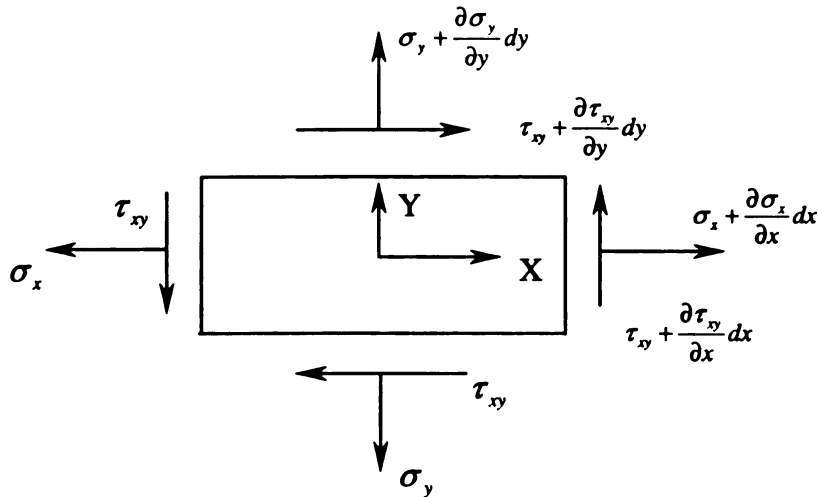


Figure 2.1. Stress components of two-dimensional problems on an element of an elastic body

A similar simplification is possible at the other extreme. Instead of a very long cylinder, we consider a very short cylinder, which can be treated as a very thin plate. It is evident that, for the very thin plate, σ_z , τ_{xz} , and τ_{yz} are zero on both faces of the plate. And they will be very small everywhere. It is therefore assumed they are all zero in the interior of the plate. The state of stress is then specified by σ_x , σ_y , and τ_{xy} only, and is called plane stress. Figure 2.1 shows these stress components in a typical element in two-dimensional problems.

There are some relationships between the states of plane strain and plane stress. For example, the equations of plane stress can be formulated and solved precisely in the same way as those for plane strain, and vice versa. The solutions of one set are derivable from those of the other merely by a change of elastic constants, for example, Young's modulus and Poisson's ratio. Hence here we only focus our attention to the state of plane strain.

2. 2 Plane Strain

Mathematically, we may describe a plane strain as one in which one of the Cartesian components of the displacement vector may be taken to be zero (with a suitable choice of axes). If we take the generators of the cylinder to be parallel to the z axis, then $u_z = 0$ where $u = (u_x, u_y, u_z)$ denotes the displacement at any point (x, y, z) .

In plane strain for which $u_z = 0$ we need consider only a section normal to the z axis. With regard to equilibrium problems, let us consider a small element of an elastic body shown in Figure 2.1.

In the absence of body forces, equilibrium in the x direction requires that:

$$\left(\sigma_x + \frac{\partial \sigma_x}{\partial x} dx \right) dy + \left(\tau_{xy} + \frac{\partial \tau_{xy}}{\partial y} dy \right) dx - \sigma_x dy - \tau_{xy} dx = 0 \quad (2.1)$$

So we have

$$\frac{\partial \sigma_x}{\partial x} + \frac{\partial \tau_{xy}}{\partial y} = 0 \quad (2.2)$$

In the y direction, we can obtain the similar equilibrium equation:

$$\frac{\partial \sigma_y}{\partial y} + \frac{\partial \tau_{xy}}{\partial x} = 0 \quad (2.3)$$

The components of strain are given by:

$$\begin{aligned} \varepsilon_x &= \frac{\partial u}{\partial x} \\ \varepsilon_y &= \frac{\partial v}{\partial y} \\ \gamma_{xy} &= \frac{\partial u}{\partial y} + \frac{\partial v}{\partial x} \end{aligned} \quad (2.4)$$

The compatibility requires

$$\frac{\partial^2 \varepsilon_x}{\partial y^2} + \frac{\partial^2 \varepsilon_y}{\partial x^2} = \frac{\partial^2 \gamma_{xy}}{\partial x \partial y} \quad (2.5)$$

If we denote the Poisson's ratio of the material by ν , its Young's modulus by E . the relations between stress and strain give

$$\begin{aligned} E\varepsilon_x &= \sigma_x - \nu(\sigma_y + \sigma_z) \\ E\varepsilon_y &= \sigma_y - \nu(\sigma_x + \sigma_z) \\ E\gamma_{xy} &= 2(1 + \nu)\tau_{xy} \end{aligned} \quad (2.6)$$

In the case of plain strain $\varepsilon_z=0$, so that the normal component of stress in the z direction is

$$\sigma_z = \nu(\sigma_x + \sigma_y) \quad (2.7)$$

Canceling out σ_z , we have

$$\begin{aligned} E\varepsilon_x &= (1 - \nu^2)\sigma_x - \nu(1 + \nu)\sigma_y \\ E\varepsilon_y &= (1 - \nu^2)\sigma_y - \nu(1 + \nu)\sigma_x \\ E\gamma_{xy} &= 2(1 + \nu)\tau_{xy} \end{aligned} \quad (2.8)$$

Substituting equations (2.8) into the two-dimensional compatibility equation (2.5), we finally obtain

$$\frac{\partial^2}{\partial y^2} [\sigma_x - \nu(\sigma_x + \sigma_y)] + \frac{\partial^2}{\partial x^2} [\sigma_y - \nu(\sigma_x + \sigma_y)] = 2 \frac{\partial^2 \tau_{xy}}{\partial x \partial y} \quad (2.9)$$

Assuming the existence of the Airy stress function χ , stresses can be expressed as

$$\begin{aligned} \sigma_x &= \frac{\partial^2 \chi}{\partial y^2} \\ \sigma_y &= \frac{\partial^2 \chi}{\partial x^2} \\ \tau_{xy} &= -\frac{\partial^2 \chi}{\partial x \partial y} \end{aligned} \quad (2.10)$$

Then the equilibrium (2.2) and (2.3) are satisfied, and the compatibility (2.9) becomes

$$\nabla^4 \chi = 0 \quad (2.11)$$

Where ∇^2 denotes the two-dimensional Laplacian operator $\frac{\partial^2}{\partial x^2} + \frac{\partial^2}{\partial y^2}$.

2.3 Solution of the Two-dimensional Biharmonic Equation

For the problems involving infinite dimension in the y-direction, it is convenient to introduce the Fourier transform of χ .

Define

$$G(x, \xi) = \int_{-\infty}^{+\infty} \chi(x, y) e^{i\xi y} dy \quad (2.12)$$

If χ satisfies the biharmonic equation (2.11), then $G(x, \xi)$ is a solution of the equation:

$$\left(\frac{d^2}{dx^2} - \xi^2 \right)^2 G = 0 \quad (2.13)$$

The general solution of equation (2.13) is given by Sneddon [8]:

$$G(x, \xi) = (A + B\xi x) \cosh(\xi x) + (C + D\xi x) \sinh(\xi x) \quad (2.14)$$

Where A, B, C, and D are functions of ξ . They are determined by the boundary conditions of the particular problems under consideration.

By the Fourier inversion theorem:

$$\begin{aligned} \text{If } \bar{f}(\alpha) &= \int_{-\infty}^{+\infty} f(y) e^{i\alpha y} dy \\ \text{then } f(y) &= \frac{1}{2\pi} \int_{-\infty}^{+\infty} \bar{f}(\alpha) e^{-i\alpha y} d\alpha \end{aligned} \quad (2.15)$$

We have:

$$\chi(x, y) = \frac{1}{2\pi} \int_{-\infty}^{+\infty} G(x, \xi) e^{-i\xi y} d\xi \quad (2.16)$$

by which the Airy stress function χ may be derived from the general expression of function $G(x, \xi)$ (2.14) by a simple integration. By using equations (2.16) and stress expressions (2.10), the stress components can be expressed in terms of G

$$\int_{-\infty}^{+\infty} \sigma_x e^{i\xi y} dy = \int_{-\infty}^{+\infty} \frac{\partial^2 \chi}{\partial y^2} e^{i\xi y} dy = -\xi^2 G \quad (2.17)$$

Similarly the second and third equations of the set (2.10) give

$$\int_{-\infty}^{+\infty} \sigma_y e^{i\xi y} dy = \frac{d^2 G}{dx^2} \quad (2.18)$$

$$\int_{-\infty}^{+\infty} \tau_{xy} e^{i\xi y} dy = i\xi \frac{dG}{dx} \quad (2.19)$$

Inverting these equations by means of the Fourier inversion theorem (2.15), we obtain the expressions

$$\sigma_x = -\frac{1}{2\pi} \int_{-\infty}^{+\infty} \xi^2 G e^{-i\xi y} d\xi \quad (2.20)$$

$$\tau_{xy} = \frac{1}{2\pi} \int_{-\infty}^{+\infty} i\xi \frac{dG}{dx} e^{-i\xi y} d\xi \quad (2.21)$$

$$\sigma_y = \frac{1}{2\pi} \int_{-\infty}^{+\infty} \frac{d^2 G}{dx^2} e^{-i\xi y} d\xi \quad (2.22)$$

According to relationships of strains and displacements (2.4) and relationships of strains and stresses (2.6), we have

$$\frac{E}{1+\nu} \frac{\partial v}{\partial y} = \sigma_y - \nu(\sigma_x + \sigma_y) \quad (2.23)$$

Then multiply by $e^{i\xi y}$, and integrate both sides to obtain:

$$\frac{E}{1+\nu} \int_{-\infty}^{+\infty} \frac{\partial v}{\partial y} e^{i\xi y} dy = (1-\nu) \int_{-\infty}^{+\infty} \sigma_y e^{i\xi y} dy - \nu \int_{-\infty}^{+\infty} \sigma_x e^{i\xi y} dy \quad (2.24)$$

According to equations (2.17) and (2.18), we obtain

$$-\frac{i\xi E}{1+\nu} \int_{-\infty}^{+\infty} v e^{i\xi y} dy = (1-\nu) \frac{d^2 G}{dx^2} + \nu \xi^2 G \quad (2.25)$$

So

$$v(x, y) = \frac{1+\nu}{2\pi E} \int_{-\infty}^{+\infty} [(1-\nu) \frac{d^2 G}{dx^2} + \nu \xi^2 G] i e^{-i\xi y} \frac{d\xi}{\xi} \quad (2.26)$$

In order to obtain the expression of normal displacement u , from the equations (2.4) and the third equation of the set (2.6), we have

$$\frac{E}{2(1+\nu)} \left(\frac{\partial v}{\partial x} + \frac{\partial u}{\partial y} \right) = \tau_{xy} \quad (2.27)$$

So

$$\frac{\partial u}{\partial y} = \frac{2(1+\nu)}{E} \tau_{xy} - \frac{\partial v}{\partial x} \quad (2.28)$$

Following the same procedure, we get

$$\int_{-\infty}^{+\infty} \frac{\partial u}{\partial y} e^{i\xi y} dy = \frac{2(1+\nu)}{E} \int_{-\infty}^{+\infty} \tau_{xy} e^{i\xi y} dy - \int_{-\infty}^{+\infty} \frac{\partial v}{\partial x} e^{i\xi y} dy \quad (2.29)$$

Finally we obtain

$$u(x, y) = \frac{1-\nu^2}{2\pi E} \int_{-\infty}^{+\infty} \left[\frac{d^3 G}{dx^3} - \left(\frac{2-\nu}{1-\nu} \right) \xi^2 \frac{dG}{dx} \right] e^{-i\xi y} \frac{d\xi}{\xi^2} \quad (2.30)$$

If the function $G(x, \xi)$ is an even function of ξ , expression of displacement u can be rewritten as:

$$u(x, y) = \frac{1-\nu^2}{\pi E} \int_0^{+\infty} \left[\frac{d^3 G}{dx^3} - \left(\frac{2-\nu}{1-\nu} \right) \xi^2 \frac{dG}{dx} \right] \cos(\xi y) \frac{d\xi}{\xi^2} \quad (2.31)$$

Similarly

$$v(x, y) = \frac{1+\nu}{\pi E} \int_0^{+\infty} \left[(1-\nu) \frac{d^2 G}{dx^2} + \nu \xi^2 G \right] \sin(\xi y) \frac{d\xi}{\xi} \quad (2.32)$$

$$\sigma_x = -\frac{1}{\pi} \int_0^{+\infty} \xi^2 G \cos(\xi y) d\xi \quad (2.33)$$

$$\tau_{xy} = \frac{1}{\pi} \int_0^{+\infty} \xi \frac{dG}{dx} \sin(\xi y) d\xi \quad (2.34)$$

$$\sigma_y = \frac{1}{\pi} \int_0^{+\infty} \frac{d^2 G}{dx^2} \cos(\xi y) d\xi \quad (2.35)$$

So, for the two-dimensional stress systems, the problem of determining the state of stresses in an elastic body under the action of given forces has been transferred into

solving the two-dimensional biharmonic equation by means of finding the function $G(x, \xi)$ in the Fourier transformed space.

Chapter 3

APPLICATION OF FOURIER TRANSFORMS TO DIFFERENT CONTACT PROBLEMS

3. 1 Formulation of the Contact Problems of the Action of Rigid Punches on an Elastic Solid

The contact problem belongs to a broad class of problems concerned with the determination of the state of stress in elastic bodies pressing against each other. The simplest case of a contact problem occurs when one of the bodies can be regarded as absolutely rigid, while the other is an elastic half-space.

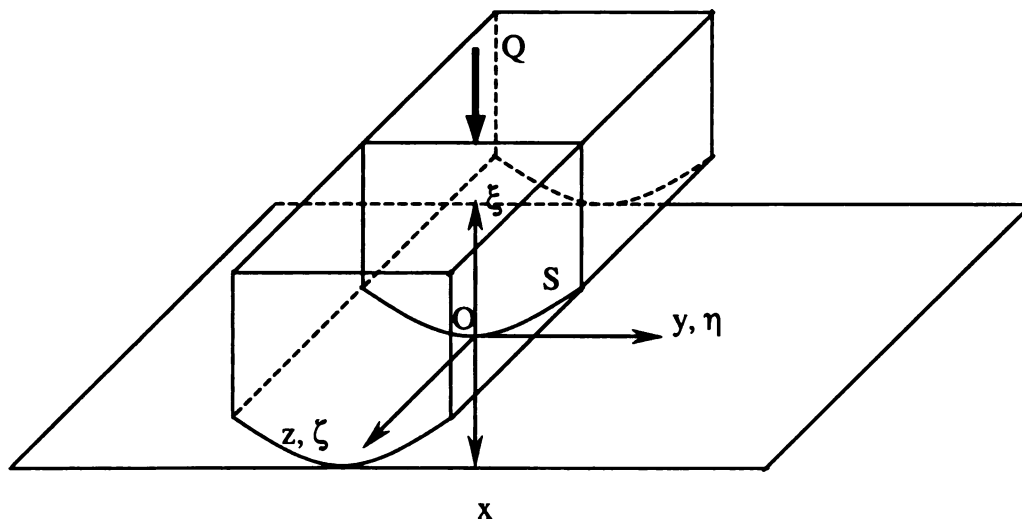


Figure 3.1 General contact problem

Figure 3.1 shows schematically a general contact problem. Let the plane bounding the elastic solid be the yOz plane and direct the positive Ox -axis into the solid. The base of the punch which presses against the solid can be either flat (the flat punch) or can have the form of a curved surface S . Let a system of coordinates ξ, η, ζ be fixed in the punch with the origin on the surfaces S and the ξ -axis directed into the punch along the normal to this surface. Initially, before the punch is loaded, the origins of the two systems $O\xi\eta\zeta$ and $Oxyz$ coincide as well as the η and y axes and ζ and z axes, while the ξ and x axes have exactly opposite directions.

In the system of axes ξ, η, ζ , let the equation of the surface S of the base of the punch be written in the form

$$\xi = \varphi(\eta, \zeta) \quad (3.1)$$

With the following conditions

$$\begin{aligned} \varphi(0,0) &= 0 \\ \left(\frac{\partial \varphi}{\partial \eta} \right)_{\eta=\zeta=0} &= 0 \\ \left(\frac{\partial \varphi}{\partial \zeta} \right)_{\eta=\zeta=0} &= 0 \end{aligned} \quad (3.2)$$

In the case of a flat punch, the equation of the plane of its base will simply be

$$\xi = 0 \quad (3.3)$$

If the shape of the punch does not change along the z -axis, and the dimension of the punch in the axis direction is very large, we can treat this kind of contact problem as plane strain problem. For simplicity, we can treat most contact problems as two-

dimensional problems. Here, the punches are assumed to be long enough, and we treat the contact problems as plane strain problems in the context.

There is a region Ω on the yz -plane containing those points which after deformation are in contact with the displaced surface S of the base of the punch. This plane region Ω is called the region of contact. Usually, the boundary conditions will be related to the undeformed surface of the elastic body, i.e., to the plane $x = 0$. Assuming the base of the punch to be perfectly smooth, we can write the boundary conditions for the shear stresses on the entire plane $x = 0$ in the form

$$\tau_{xy} = 0 \quad (3.4)$$

The normal stress σ_x vanishes on the plane $x = 0$ outside the region of contact Ω :

$$\sigma_x = 0 \quad (\textit{outside } \Omega) \quad \textit{for } x = 0 \quad (3.5)$$

At the points of the region Ω , the elastic medium is subject to the action of a compressive load $p(y)$, the distribution of which is unknown beforehand and must be found from the solution of the problem:

$$\sigma_x = -p(y) \quad (\textit{inside } \Omega) \quad \textit{for } x = 0 \quad (3.6)$$

Under these conditions, equilibrium of the punch can be achieved by application to the punch of a force Q parallel to the x -axis. Then the equilibrium equation of the punch will be

$$Q = \int_{\Omega} p(y) dy \quad (3.7)$$

Under the action of the force Q , the punch undergoes a vertical translation, and here we do not consider the rotation. The indentation δ will be parallel to the x -axis. The x -

direction displacement of the points on the surface S of the punch base can be expressed in terms of δ . Noting that the coordinates of the origin of the ξ, η, ζ system in the xyz system are $(0, 0, \delta)$. Thus, the required boundary condition for the normal displacement u is:

$$u = \delta - \varphi(y) \quad (\text{inside } \Omega) \quad \text{for } x = 0 \quad (3.8)$$

For the flat punch, this condition simplifies to the form:

$$u = \delta \quad (\text{inside } \Omega) \quad \text{for } x = 0 \quad (3.9)$$

Thus the question of the effect of a rigid punch on an elastic solid has been reduced to the consideration of the following mixed boundary value problem of the theory of elasticity:

1. the shear stresses τ_{xy} vanish on the entire plane $x = 0$,
2. outside the region Ω of this plane, the normal stress σ_x vanishes,
3. the values of the normal displacement u of the points in the region Ω are prescribed.

This statement can be interpreted thus: the points of the plane $x = 0$ which belong to the region Ω undergo normal displacement u in accordance with a given law (3.8) for which the region Ω must be subjected to a normal pressure $p(y)$, the distribution of which is initially unknown. A vertical force Q must be applied to the punch, in order to maintain it in equilibrium during the indentation.

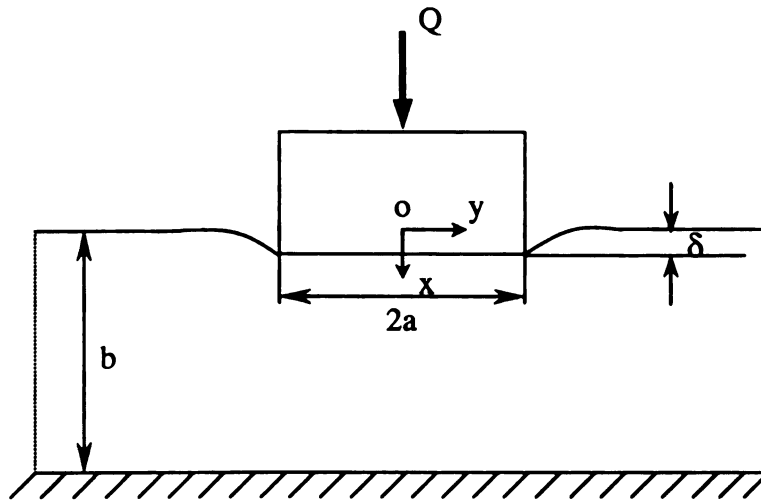


Figure 3.2 Conforming contact problem

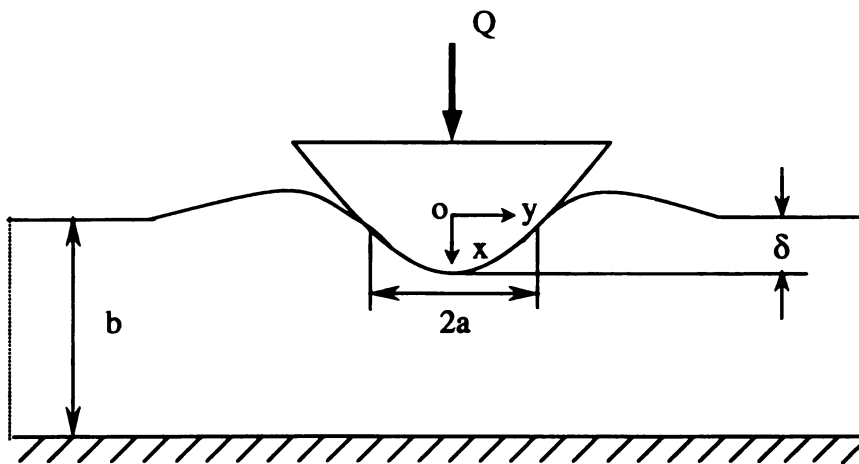


Figure 3.3 Non-conforming contact problem

There are two distinct classes of problems relating to indentation by a frictionless punch. They are shown in Figure 3.2 and Figure 3.3. In the first kind of indentation, called conforming contact problem, there is complete contact between the punch and the elastic

solid over a specified contact region, in the sense that the normal displacement of the elastic solid at the boundary matches the profile of the rigid punch. Such problems are characterized by a contact pressure which has a singularity at the ends of the contact region. In the second kind, called non-conforming contact problem, the extent of the contact region, i.e. the extent of the region over which the normal displacement of the elastic solid matches the profile of the punch, is initially unknown. Cases of non-conforming contact problems are characterized by a contact pressure which is zero at the ends of the contact region.

3. 2 Conforming Contact Problem

For the conforming contact problem, the contact region is prescribed. For this class of contact problems, the contact pressure is unknown, and needs to be solved. Taking a flat punch as an example, we introduce a numerical solution procedure to solve the contact problem. Considering the influence of different geometries of the elastic solid, we divide the elastic solid into infinity, single-layer, and multi-layer according to their physical properties. In the meantime, the infinite elastic solid can be treated as a special example of the single-layered solid. So the problem of conforming contact is finally categorized into two cases: two symmetrical flat punches on a single-layered elastic solid and two symmetrical flat punches on a multi-layered elastic solid.

3. 2. 1 A Numerical Procedure for Solving Contact Pressure

Let us take a look at the expression of normal displacement u (2.31):

$$u(x, y) = \frac{1-\nu^2}{\pi E} \int_0^{+\infty} \left[\frac{d^3 G}{dx^3} - \left(\frac{2-\nu}{1-\nu} \right) \xi^2 \frac{dG}{dx} \right] \cos(\xi y) \frac{d\xi}{\xi^2}$$

We see, for the rigid punch, the normal component u of the surface displacement is prescribed within the contact area. From the expression of displacement u , we can use a numerical method to obtain the contact pressure.

First, considering the surface deflection due to a unit uniform pressure, if we assume that the half width is α , the magnitude of uniform pressure is $\frac{1}{2\alpha}$. Define $\bar{p}(\xi)$ as:

$$\begin{aligned} \bar{p}(\xi) &= \int_0^{+\infty} p(y) \cos(\xi y) dy \\ &= \frac{1}{2\alpha} \int_0^{\alpha} \cos(\xi y) dy = \frac{\sin(\xi \alpha)}{2\xi \alpha} \end{aligned} \quad (3.10)$$

For the uniform pressure, the displacement u may be denoted in terms of function $K(y)$.

For the plane strain problem, u can be defined as

$$\bar{u}(y) = \frac{1-\nu^2}{\pi E} K(y) \quad (3.11)$$

Where

$$K(y) = \int_0^{+\infty} \left[\frac{d^3 G}{dx^3} - \left(\frac{2-\nu}{1-\nu} \right) \xi^2 \frac{dG}{dx} \right] \cos(\xi y) \frac{d\xi}{\xi^2} \quad (3.12)$$

So in the contact area, if the contact pressure is a function $p(y)$, then we know the displacement u for the arbitrary contact pressure $p(y)$ is

$$\frac{1-\nu^2}{\pi E} \int_{-a}^{+a} p(\eta)K(|y-\eta|)d\eta = u(y) \quad (3.13)$$

Where

a: half contact length

Further we have

$$\frac{1-\nu^2}{\pi E} \left[\int_{-a}^0 p(\eta)K(|y-\eta|)d\eta + \int_0^{+a} p(\eta)K(|y-\eta|)d\eta \right] = u(y) \quad (3.14)$$

Define

$$t = -\eta \quad (3.15)$$

We can rewrite the equation (3.14) into

$$\frac{1-\nu^2}{\pi E} \left[\int_{+a}^0 p(-t)K(|y+t|)d(-t) + \int_0^{+a} p(\eta)K(|y-\eta|)d\eta \right] = u(y) \quad (3.16)$$

If the distribution of contact pressure $p(y)$ is even, we have

$$\frac{1-\nu^2}{\pi E} \left\{ \int_0^{+a} p(\eta)[K(|y-\eta|) + K(|y+\eta|)]d\eta \right\} = u(y) \quad (3.17)$$

Define

$$Q(\beta, \eta) = K(|\beta-\eta|) + K(|\beta+\eta|) \quad (3.18)$$

We obtain

$$\frac{(1-\nu^2)}{\pi E} \int_0^a Q(y, \eta)p(\eta)d\eta = u(y) \quad (3.19)$$

With regard to the half contact area, we can divide it into n small areas, and assume each small area is loaded with a uniform pressure p_i . Figure 3.4 visualizes the idea.

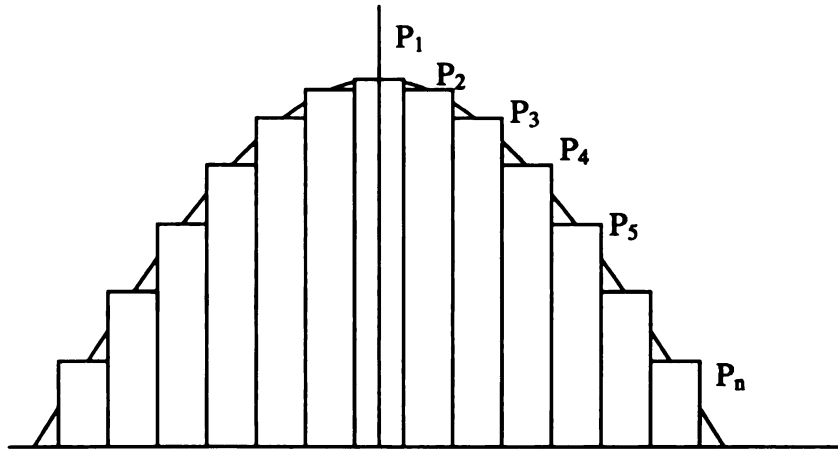


Figure 3.4 The trapezoidal rule

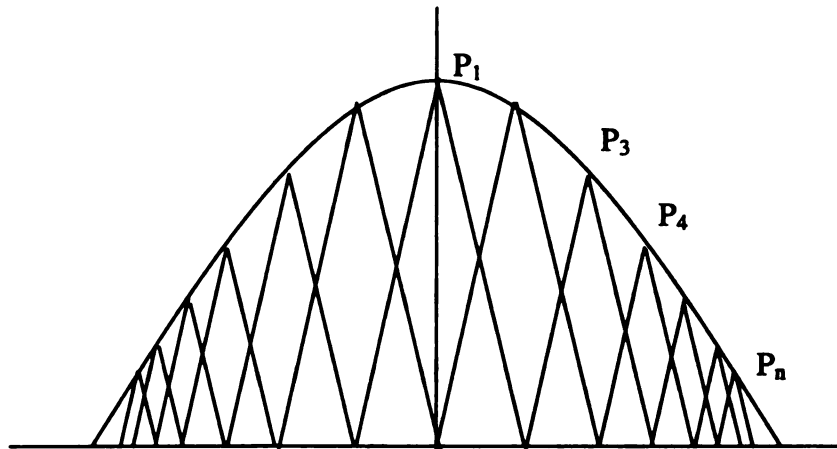


Figure 3.5 The triangular rule

Figure 3.5 illustrates another numerical contact pressure kernel. It utilizes the triangular distribution of contact pressure instead of the common rectangular assumption. The general numerical procedure is the same for both rectangular and triangular kernels.

Besides, they can obtain very similar results. Even though using the triangular one can save about 5% computer calculation time comparing with using rectangular kernel, it creates more errors. We choose to use rectangular kernel in the context instead.

Dividing the pressure profile in discrete

$$p_i \quad i = 1, n \quad (3.20)$$

So the following is the numerical solution equation

$$\frac{(1-\nu^2)}{\pi E} \sum_{i=1}^n Q(y_j, \eta_i) p(\eta_i) = u_j \quad j = 1, n \quad (3.21)$$

Where

$$Q(y_j, \eta_i) = K(|y_j - \eta_i|) + K(|y_j + \eta_i|) \quad (3.22)$$

$$K(|y_j - \eta_i|) = \int_0^{+\infty} \left[\frac{d^3 G}{dx^3} - \left(\frac{2-\nu}{1-\nu} \right) \xi^2 \frac{dG}{dx} \right] \cos(\xi |y_j - \eta_i|) \frac{d\xi}{\xi^2} \quad (3.23)$$

Equation (3.21) can be written as the following matrix format. By the matrix inversion, we can solve the equation and obtain numerical solutions of the contact pressure.

$$\frac{(1-\nu^2)}{\pi E} \begin{bmatrix} Q_{11} & Q_{12} & \cdots & Q_{1n-1} & Q_{1n} \\ Q_{21} & Q_{22} & \cdots & Q_{2n-1} & Q_{2n} \\ \vdots & \vdots & \ddots & \vdots & \vdots \\ Q_{n-11} & Q_{n-12} & \cdots & Q_{n-1n-1} & Q_{n-1n} \\ Q_{n1} & Q_{n2} & \cdots & Q_{nn-1} & Q_{nn} \end{bmatrix} \begin{Bmatrix} p_1 \\ p_2 \\ \vdots \\ p_{n-1} \\ p_n \end{Bmatrix} = \begin{Bmatrix} u_1 \\ u_2 \\ \vdots \\ u_{n-1} \\ u_n \end{Bmatrix} \quad (3.24)$$

In the following, we will deal with how to utilize the numerical solution procedure to solve various contact problems, and get the practical solutions. Prior to utilization, the accuracy and efficiency of the numerical procedure need to be considered.

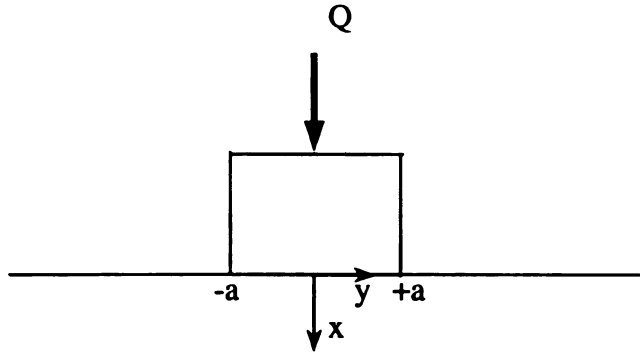


Figure 3.6 The contact problem between a rigid flat punch and a half space

Let us consider the contact problem of a rigid flat punch pressing on a half space that is shown schematically in Figure 3.6. The boundary conditions are:

On $x = 0$:

$$\begin{aligned} \sigma_x(0, y) &= -p(y) & |y| \leq a \\ \sigma_x(0, y) &= 0 & |y| > a \end{aligned} \quad (3.25)$$

$$\tau_{xy}(0, y) = 0 \quad -\infty < y < +\infty \quad (3.26)$$

$$u(0, y) = \delta \quad (3.27)$$

When $x \rightarrow +\infty$:

$$\sigma_x = \sigma_y = \tau_{xy} = 0 \quad (3.28)$$

Taking

$$G(x, \xi) = (A + Bx)e^{-|\xi|x} + (C + Dx)e^{+|\xi|x} \quad (3.29)$$

and considering the boundary condition (3.28), we have

$$C = D = 0 \quad (3.30)$$

Using the boundary conditions (3.25) and (3.26), and expressions of stresses (2.17) and (2.19), we can finally obtain

$$G(x, \xi) = \frac{\bar{p}(\xi)}{\xi^2} (1 + |\xi|x) e^{-|\xi|x} \quad (3.31)$$

where $\bar{p}(\xi)$ is given by equation (3.10).

When $\bar{p}(\xi)$ is an even function of ξ , the normal displacement u can be written as

$$u(x, y) = \frac{(1 - \nu^2)}{\pi E} \int_0^{+\infty} \left[2 + \frac{\xi x}{1 - \nu} \right] \bar{p}(\xi) e^{-\xi x} \frac{\cos(\xi y)}{\xi} d\xi \quad (3.32)$$

Utilizing the boundary condition (3.27) and considering the numerical procedure mentioned above, we can obtain numerical solution of the contact pressure. Where the kernel K is:

$$K(x, y) = \int_0^{+\infty} \left[2 + \frac{\xi x}{1 - \nu} \right] \bar{p}(\xi) e^{-\xi x} \frac{\cos(\xi y)}{\xi} d\xi \quad (3.33)$$

On the surface, according to the coordinates shown in Figure 3.6 $x = 0$, we have

$$K(x, y) = \int_0^{+\infty} 2\bar{p}(\xi) \frac{\cos(\xi y)}{\xi} d\xi \quad (3.34)$$

For the contact problem of a rigid flat punch pressing on a half space, the exact solution is available [26]

$$p(y) = \frac{Q}{\pi \sqrt{a^2 - y^2}} \quad (3.35)$$

Where

Q: total load

a: half contact length

So a comparison can be made between our solution and the exact solution to verify the numerical solution procedure.

The development of modern computer makes the large numerical calculation practical. In this work, mathematica 4.1 software [27] are used to write program codes and do the numerical calculations.

From the graph of Figure 3.7, we see the effect of the point number that we are choosing to do the simulation on the distribution of the contact pressure. A satisfactory solution can be obtained by using 40 or 50 points in the half contact area to do the numerical calculation. Basically the exact solution and numerical solution match well except the regions that are near the end of the contact. The contact pressure has a singularity at this area.

Through the comparison of results of 40 points and 50 points simulations of contact pressure in the half contact length. The calculation demonstrates that by using 40 and 50 points to simulate the contact pressure in the half contact length the pressure distributions are very similar, though the solution of 50 points is a bit closer to the exact solution. However, using 40 points saves about 30% computation time. Which can greatly increase the efficiency of work. Therefore, 40 points simulation is used in the context.

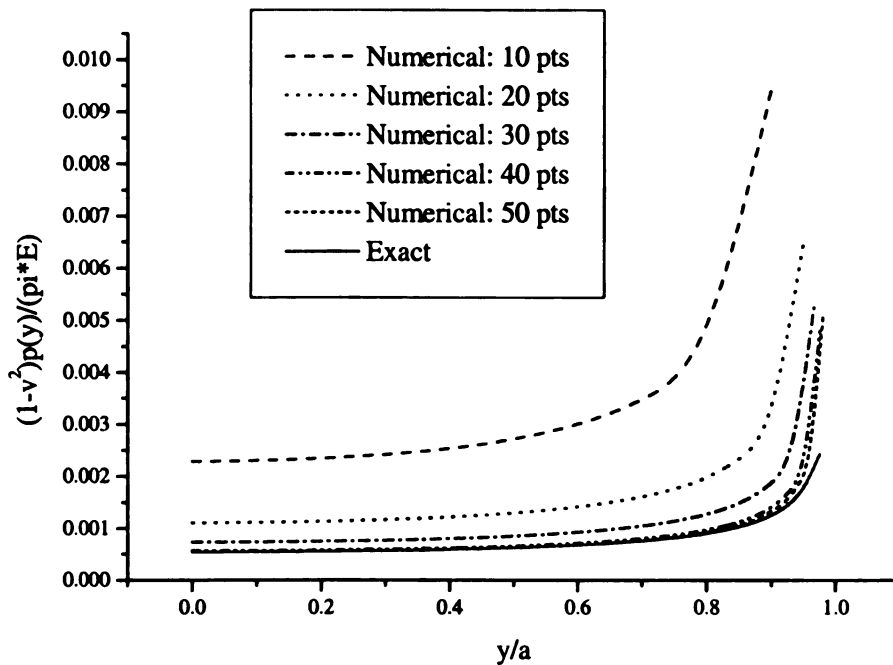


Figure 3.7 Comparison between numerical solution and exact solution of contact problem by a rigid flat punch on half space

3. 2. 2 Rigid Flat Punches on a Single-layered Elastic Solid

Figure 3.8 depicts the problem of an elastic solid of thickness $2b$ compressed between two same rigid flat punches. If the coordinate axes are chosen in such a way that the solid has the plane $x = 0$ as its middle surface, on which the shear stress τ_{xy} and the vertical displacement u are zero because of symmetry, the problem is therefore equivalent to the indentation of a layer of thickness b resting on a smooth rigid half space $-\infty < x < 0$.

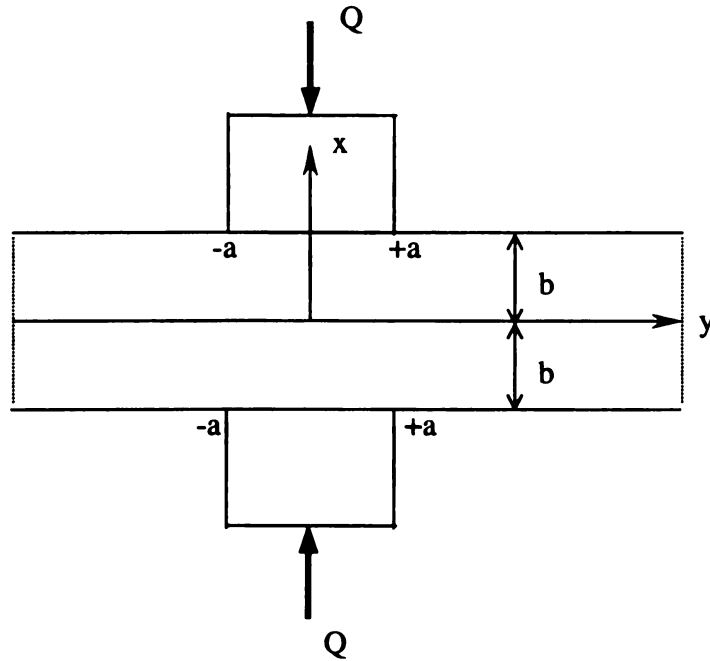


Figure 3.8 Rigid flat punches on a single-layered elastic solid

The boundary conditions for this problem are:

On $x = \pm b$:

$$\begin{aligned} \sigma_x(\pm b, y) &= -p(y) & |y| \leq a \\ \sigma_x(\pm b, y) &= 0 & |y| > a \end{aligned} \quad (3.36)$$

$$\tau_{xy}(\pm b, y) = 0 \quad -\infty < y < +\infty \quad (3.37)$$

$$u(\pm b, y) = \pm b \mp \delta \quad (3.38)$$

Where

$p(y)$: unknown contact pressure

a : half contact length

δ : indentation depth of the rigid flat punches

From equation (2.14), the general expression of function $G(x, \xi)$ is:

$$G(x, \xi) = (A + B\xi x) \cosh(\xi x) + (C + D\xi x) \sinh(\xi x)$$

Where A, B, C, and D are functions of ξ .

According to the general expression of function $G(x, \xi)$, normal stress expression (2.17) and boundary condition (3.36), we have

$$-\int_{-a}^{+a} p(y) e^{i\xi y} dy = -\xi^2 [(A + B\xi b) \cosh(\xi b) + (C + D\xi b) \sinh(\xi b)] \quad (3.39)$$

Since the rigid punches are symmetrical, the contact pressure $p(y)$ is even. We get

$$2 \int_0^{+a} p(y) \cos(\xi y) dy = \xi^2 [(A + B\xi b) \cosh(\xi b) + (C + D\xi b) \sinh(\xi b)] \quad (3.40)$$

From the shear stress expression (2.19) and boundary condition (3.37), we obtain

$$\int_{-\infty}^{+\infty} \tau_{xy} e^{i\xi y} dy = i\xi \frac{dG}{dx} = 0 \quad (3.41)$$

Which leads to

$$(B + C + D\xi b) \xi \cosh(\xi b) + (A + D + B\xi b) \xi \sinh(\xi b) = 0 \quad (3.42)$$

On the $x = -b$, because of symmetry, the contact pressure $p(y)$ is even. Similarly, according to general expression of function $G(x, \xi)$ (2.14), stress expressions (2.17), (2.19), and boundary conditions (3.36), (3.37), we have

$$2 \int_0^{+a} p(y) \cos(\xi y) dy = \xi^2 [(A - B\xi b) \cosh(\xi b) - (C - D\xi b) \sinh(\xi b)] \quad (3.43)$$

$$(B + C - D\xi b) \xi \cosh(\xi b) - (A + D - B\xi b) \xi \sinh(\xi b) = 0 \quad (3.44)$$

From the equations (3.40) and (3.43), we obtain

$$C = -B\xi b \frac{\cosh(\xi b)}{\sinh(\xi b)} \quad (3.45)$$

From the equations (3.42) and (3.44), we have

$$A = -D[\xi b \frac{\cosh(\xi b)}{\sinh(\xi b)} + 1] \quad (3.46)$$

Define

$$\bar{p}(\xi) = \int_0^{\pi} p(y) \cos(\xi y) dy \quad (3.47)$$

Finally, we obtain:

$$B = C = 0 \quad (3.48)$$

$$D = -\frac{4 \sinh(\xi b)}{2\xi b + \sinh(2\xi b)} \frac{\bar{p}(\xi)}{\xi^2} \quad (3.49)$$

$$A = \frac{4[\sinh(\xi b) + \xi b \cosh(\xi b)]}{2\xi b + \sinh(2\xi b)} \frac{\bar{p}(\xi)}{\xi^2} \quad (3.50)$$

Then the function $G(x, \xi)$ can be expressed as:

$$G(x, \xi) = \frac{4[\sinh(\xi b) + \xi b \cosh(\xi b)]}{2\xi b + \sinh(2\xi b)} \frac{\bar{p}(\xi)}{\xi^2} \cosh(\xi x) - \frac{4 \sinh(\xi b)}{2\xi b + \sinh(2\xi b)} \frac{\bar{p}(\xi)}{\xi^2} \xi x \sinh(\xi x) \quad (3.51)$$

Until now we have known the expression of function $G(x, \xi)$, we can determine the distribution of stress in the interior of the strip according to expressions (2.20), (2.21) and (2.22), if the contact pressure $p(y)$ is known too. But usually we do not know the contact pressure in advance. In order to get the contact pressure in the contact area, the new numerical procedure that is introduced above is used to solve this problem in the following.

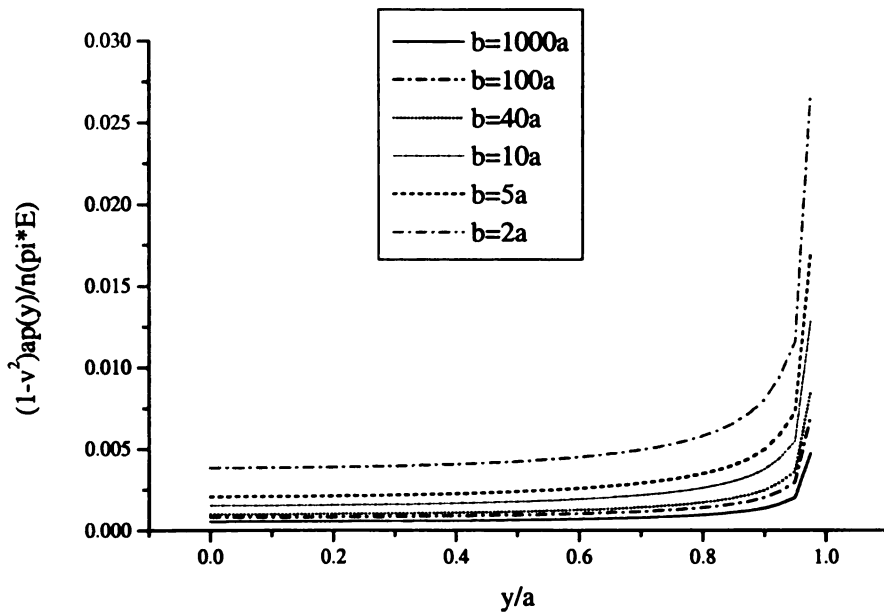


Figure 3.9 Contact pressure variations for various thicknesses of the solid

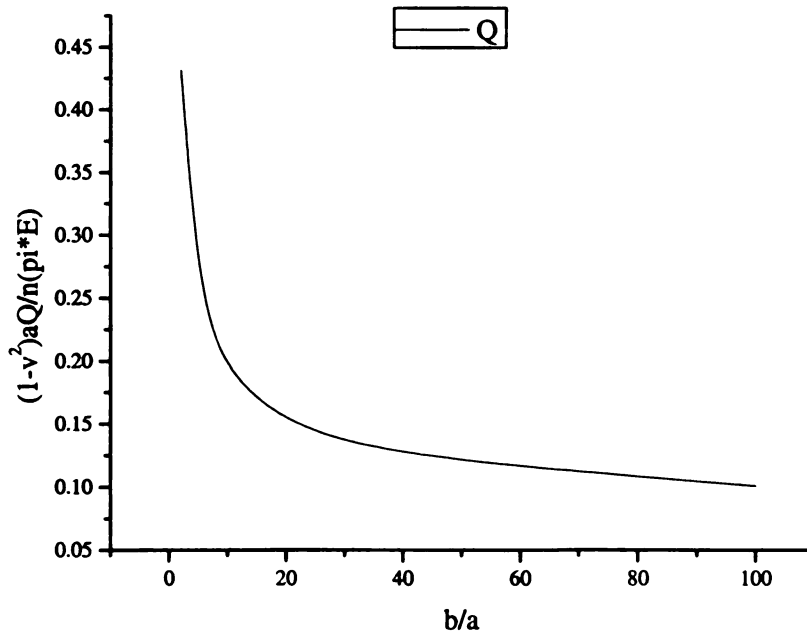


Figure 3.10 Total loads versus thicknesses of the solid

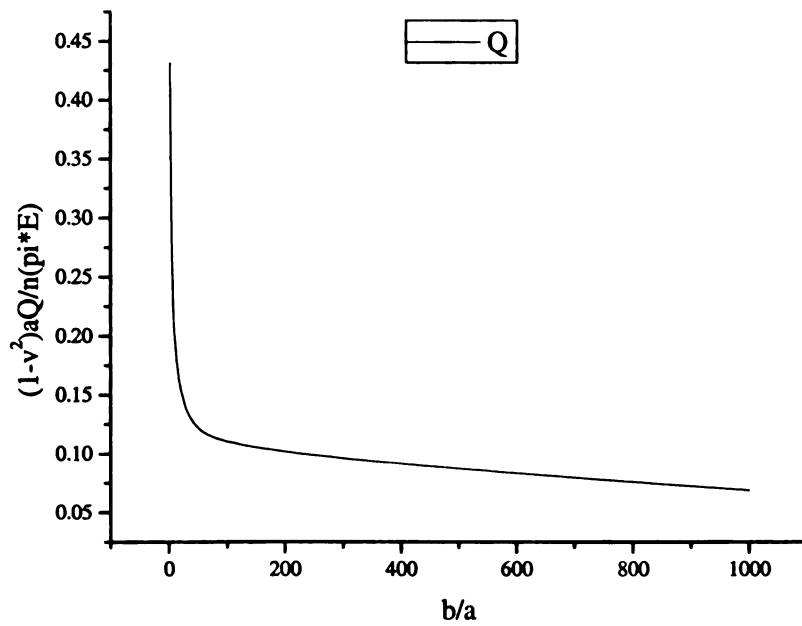


Figure 3.11 Total loads versus more thicknesses of the solid

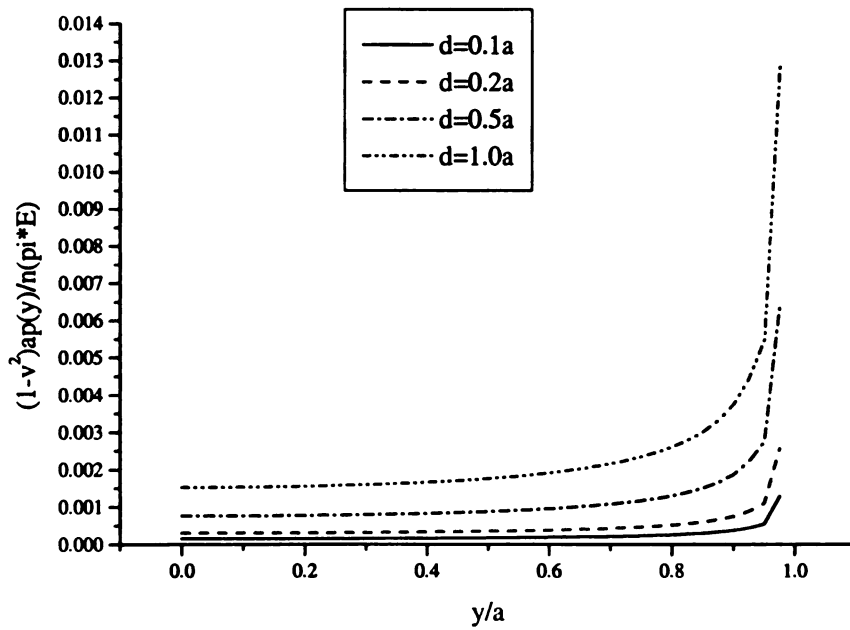


Figure 3.12 Contact pressure variations for different indentation depths

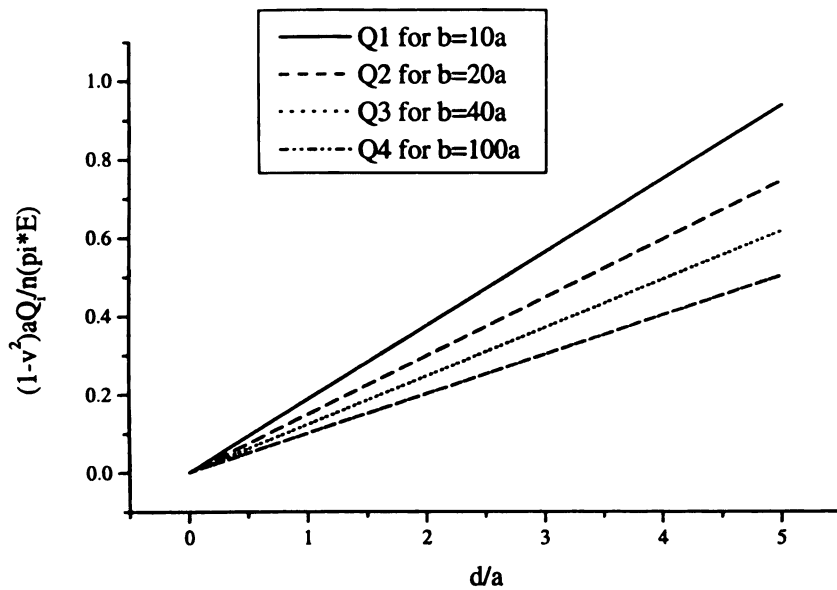


Figure 3.13 Total load versus indentation

Figure 3.9 shows that the effect of layer thickness on contact pressure. In order to study the effect of thickness, other properties of the elastic solid, such as Young's modulus, Poisson's ratio, and the indentation depth, are kept same for different thicknesses of the elastic solid. The contact pressure increases as the decrease of the thickness of the solid.

For different thicknesses of the solid, in order to reach the same indentation depth, different total loads Q are needed. Figure 3.10 and Figure 3.11 present the phenomena. The relationship between total loads and thicknesses of the solid is nonlinear. When the solid is thin, the necessary total load will change greatly to reach the same indentation depth once the thickness of the solid is only changed a little bit. But, as the thickness of the solid turns thicker and thicker, the effect of the thickness of the elastic solid on the total load will become smaller and smaller. The trend is illustrated in Figure 3.11 clearly.

The effect of indentation is obvious. Figure 3.12 shows the general trend for this kind of problem corresponding to a special layer thickness. As the increase of indentation depth, more contact pressure is expected in the contact area.

Further, the relationship between total loads and different indentation depths can be found with the case of classical linear elastic theory. From the derivation, we know, for the rigid flat punch

$$\frac{(1-\nu^2)}{\pi E} \int_0^a Q(y, \eta) p(\eta) d\eta = u(y) = \delta \quad (3.52)$$

Total load is

$$Q = 2 \int_0^a p(y) dy \quad (3.53)$$

Since the kernel $Q(y, \eta)$ is only related to the known contact length, and is not related to the indentation depth, we have such a relationship

$$Q \propto \delta \quad (3.54)$$

Figure 3.13 confirms the linear relationship. For various indentation depths, corresponding total loads can be obtained easily from the plot. Besides we can find the effect of the thickness of the elastic solid. Considering the same material properties, the influence of the thickness on total loads to obtain the same indentation depth is quite considerable. The thicker the elastic solid, the smaller is total load needed to obtain same amount of indentation depth. Which verifies the conclusion shown in Figure 3.10 and Figure 3.11 again.

3. 2. 3 Rigid Flat Punches on a Multi-layered Elastic Solid

The contact problem of layered elastic solids has been of considerable interest in various fields of science and engineering. A number of solutions to the problem of an elastic layer on a rigid substrate have been presented in the literature. However, solutions to the contact problem of multi-layered elastic solids are seldom given. The objective of this part is to obtain a generalized plane strain solution to the contact problem of a multi-layered solid and rigid flat punches.

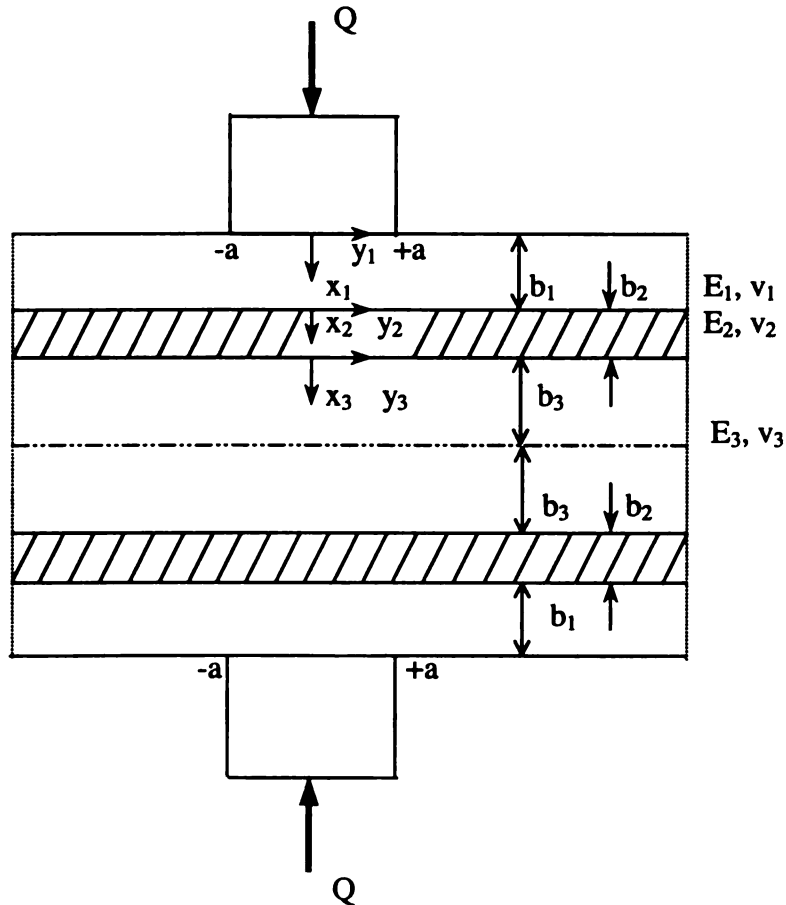


Figure 3.14 rigid punches on a multi-layered elastic solid

Figure 3.14 depicts schematically a multi-layered elastic solid pressed by two symmetrical flat punches. It is assumed that there is perfect adherence between layers, and the contact of the indenter is frictionless. For simplicity, we let layer 1 and layer 3 have same material properties, such as Young's modulus and Poisson's ratio, which can be different if required. So we can concentrate on the effect of the middle layer 2 on the distribution of the contact pressure.

It is now well known that the contact pressure distribution of a layered elastic system deviates significantly from that given by Hertzian theory. Therefore, as the pressure distribution directly affects the stress-strain fields, it is crucial to obtain a realistic contact pressure profile. In the preceding part, the solutions for a single-layered elastic solid pressed by rigid flat punches are investigated; the contact pressure distributions are obtained for various indentation depths and layer thicknesses. In the following, the numerical procedure will be refined and applied into the contact problem of a multi-layered elastic solid pressed by flat punches. Solutions describing the contact pressures for different contact geometries, layer properties and thicknesses will be obtained.

From the Figure 3.14 using subscript 1 for layer 1 and 2 for layer2, etc., the boundary conditions for the contact problem are given by:

On $x_1 = 0$:

$$\begin{aligned} \sigma_{x_1} &= -p(y_1) & |y_1| \leq a \\ \sigma_{x_1} &= 0 & |y_1| > a \end{aligned} \quad (3.55)$$

$$\tau_{x_1 y_1} = 0 \quad -\infty < y_1 < +\infty \quad (3.56)$$

On $x_1 = b_1$ and $x_2 = 0$:

$$\begin{aligned}
 \sigma_{x_1} &= \sigma_{x_2} \\
 \tau_{x_1 y_1} &= \tau_{x_2 y_2} \\
 u_1 &= u_2 \\
 v_1 &= v_2
 \end{aligned} \tag{3.57}$$

On $x_2 = b_2$ and $x_3 = 0$:

$$\begin{aligned}
 \sigma_{x_2} &= \sigma_{x_3} \\
 \tau_{x_2 y_2} &= \tau_{x_3 y_3} \\
 u_2 &= u_3 \\
 v_3 &= v_3
 \end{aligned} \tag{3.58}$$

On $x_3 = b_3$, because of symmetry:

$$\begin{aligned}
 \tau_{x_3 y_3} &= 0 \\
 u_3 &= 0
 \end{aligned} \tag{3.59}$$

Since the punch is flat and rigid, we know:

$$u_1(y_1) = \delta \quad |y_1| \leq a \tag{3.60}$$

Where

δ : indentation depth

a : half contact length

On $x_1 = 0$, according to the general expression of function $G(x, \xi)$ (2.14), normal stress equation (2.17), and boundary conditions (3.55), parameter A_1 can be expressed as:

$$- \int_{-a}^{+a} p(y_1) e^{i\delta y_1} dy_1 = -\xi^2 A_1 \tag{3.61}$$

Assuming $p(y_1)$ is even function, equation (3.61) can be rewritten as:

$$2 \int_0^{+a} p(y_1) \cos(\xi y_1) dy_1 = \xi^2 A_1 \quad (3.62)$$

Define:

$$\bar{p}(\xi) = \int_0^{+a} p(y_1) \cos(\xi y_1) dy_1 \quad (3.63)$$

So

$$A_1 = \frac{2\bar{p}(\xi)}{\xi^2} \quad (3.64)$$

From the shear stress expression (2.19) and boundary condition (3.56), we have

$$\frac{dG_1}{dx_1} = 0 \quad (3.65)$$

Which concludes:

$$B_1 + C_1 = 0 \quad (3.66)$$

On $x_1 = b_1$, and $x_2 = 0$, from boundary conditions (3.57), due to the matching stress conditions between layer1 and layer 2, we obtain

$$G_1|_{x_1=b_1} = G_2|_{x_2=0} \quad (3.67)$$

$$\left. \frac{dG_1}{dx_1} \right|_{x_1=b_1} = \left. \frac{dG_2}{dx_2} \right|_{x_2=0} \quad (3.68)$$

That is

$$A_2 = (A_1 + B_1 \xi b_1) \cosh(\xi b_1) + (C_1 + D_1 \xi b_1) \sinh(\xi b_1) \quad (3.69)$$

$$B_2 + C_2 = (B_1 + C_1 + D_1 \xi b_1) \cosh(\xi b_1) + (A_1 + D_1 + B_1 \xi b_1) \sinh(\xi b_1) \quad (3.70)$$

Considering the boundary conditions (3.57), the matching displacements at the interface

are:

$$\frac{1-\nu_1^2}{E_1} \left[\frac{d^3 G_1}{dx_1^3} - \frac{2-\nu_1}{1-\nu_1} \xi^2 \frac{dG_1}{dx_1} \right]_{x_1=b_1} = \frac{1-\nu_2^2}{E_2} \left[\frac{d^3 G_2}{dx_2^3} - \frac{2-\nu_2}{1-\nu_2} \xi^2 \frac{dG_2}{dx_2} \right]_{x_2=0} \quad (3.71)$$

$$\frac{1-\nu_1^2}{E_1} \left[\frac{d^2 G_1}{dx_1^2} + \frac{\nu_1}{1-\nu_1} \xi^2 G_1 \right]_{x_1=b_1} = \frac{1-\nu_2^2}{E_2} \left[\frac{d^2 G_2}{dx_2^2} + \frac{\nu_2}{1-\nu_2} \xi^2 G_2 \right]_{x_2=0} \quad (3.72)$$

Define:

$$\lambda_1 = \frac{2-\nu_1}{1-\nu_1} \quad (3.73)$$

$$\lambda_2 = \frac{2-\nu_2}{1-\nu_2} \quad (3.74)$$

$$\omega_1 = \frac{\nu_1}{1-\nu_1} \quad (3.75)$$

$$\omega_2 = \frac{\nu_2}{1-\nu_2} \quad (3.76)$$

$$H_1 = \frac{1-\nu_1^2}{E_1} \quad (3.77)$$

$$H_2 = \frac{1-\nu_2^2}{E_2} \quad (3.78)$$

Modified boundary conditions (3.71) and (3.72) can be rewritten as:

$$\begin{aligned} & H_1 \{ [(3-\lambda_1)B_1 + (1-\lambda_1)(C_1 + D_1 \xi b_1)] \cosh(\xi b_1) \\ & + [(3-\lambda_1)D_1 + (1-\lambda_1)(A_1 + B_1 \xi b_1)] \sinh(\xi b_1) \} \\ & = H_2 [(3-\lambda_2)B_2 + (1-\lambda_2)C_2] \end{aligned} \quad (3.79)$$

$$\begin{aligned} & H_1 \{ [2D_1 + (1+\omega_1)(A_1 + B_1 \xi b_1)] \cosh(\xi b_1) \\ & + [2B_1 + (1+\omega_1)(C_1 + D_1 \xi b_1)] \sinh(\xi b_1) \} \\ & = H_2 [2D_2 + (1+\omega_2)A_2] \end{aligned} \quad (3.80)$$

Following the same steps, utilizing the boundary conditions on the $x_2 = b_2$, $x_3 = 0$, and $x_3 = b_3$, finally we can obtain twelve equations for the twelve constants of the airy functions.

$$A_1 = \frac{2\bar{p}(\xi)}{\xi^2} \quad (3.81)$$

$$B_1 + C_1 = 0 \quad (3.82)$$

$$\cosh(\xi b_1)A_1 + \xi b_1 \cosh(\xi b_1)B_1 + \sinh(\xi b_1)C_1 + \xi b_1 \sinh(\xi b_1)D_1 - A_2 = 0 \quad (3.83)$$

$$\sinh(\xi b_1)A_1 + [\xi b_1 \sinh(\xi b_1) + \cosh(\xi b_1)]B_1 + \cosh(\xi b_1)C_1 + [\xi b_1 \cosh(\xi b_1) + \sinh(\xi b_1)]D_1 - B_2 - C_2 = 0 \quad (3.84)$$

$$H_1(1 - \lambda_1) \sinh(\xi b_1)A_1 + H_1[(3 - \lambda_1) \cosh(\xi b_1) + (1 - \lambda_1)\xi b_1 \sinh(\xi b_1)]B_1 + H_1(1 - \lambda_1) \cosh(\xi b_1)C_1 + H_1[(3 - \lambda_1) \sinh(\xi b_1) + (1 - \lambda_1)\xi b_1 \cosh(\xi b_1)]D_1 - H_2(3 - \lambda_2)B_2 - H_2(1 - \lambda_2)C_2 = 0 \quad (3.85)$$

$$H_1(1 + \omega_1) \cosh(\xi b_1)A_1 + H_1[(1 + \omega_1)\xi b_1 \cosh(\xi b_1) + 2 \sinh(\xi b_1)]B_1 + H_1(1 + \omega_1) \sinh(\xi b_1)C_1 + H_1[(1 + \omega_1)\xi b_1 \sinh(\xi b_1) + 2 \cosh(\xi b_1)]D_1 - H_2(1 + \omega_2)A_2 - 2H_2D_2 = 0 \quad (3.86)$$

$$\cosh(\xi b_2)A_2 + \xi b_2 \cosh(\xi b_2)B_2 + \sinh(\xi b_2)C_2 + \xi b_2 \sinh(\xi b_2)D_2 - A_3 = 0 \quad (3.87)$$

$$\sinh(\xi b_2)A_2 + [\xi b_2 \sinh(\xi b_2) + \cosh(\xi b_2)]B_2 + \cosh(\xi b_2)C_2 + [\xi b_2 \cosh(\xi b_2) + \sinh(\xi b_2)]D_2 - B_3 - C_3 = 0 \quad (3.88)$$

$$H_2(1 - \lambda_2) \sinh(\xi b_2)A_2 + H_2[(3 - \lambda_2) \cosh(\xi b_2) + (1 - \lambda_1)\xi b_1 \sinh(\xi b_1)]B_1 + H_2(1 - \lambda_1) \cosh(\xi b_1)C_1 + H_2[(3 - \lambda_1) \sinh(\xi b_1) + (1 - \lambda_1)\xi b_1 \cosh(\xi b_1)]D_1 - H_2(3 - \lambda_2)B_2 - H_2(1 - \lambda_2)C_2 = 0 \quad (3.89)$$

$$H_2(1 + \omega_2) \cosh(\xi b_2)A_2 + H_2[(1 + \omega_2)\xi b_2 \cosh(\xi b_2) + 2 \sinh(\xi b_2)]B_2 + H_2(1 + \omega_2) \sinh(\xi b_2)C_2 + H_2[(1 + \omega_2)\xi b_2 \sinh(\xi b_2) + 2 \cosh(\xi b_2)]D_2 - H_3(1 + \omega_3)A_3 - 2H_3D_3 = 0 \quad (3.90)$$

$$\sinh(\xi b_3)A_3 + [\xi b_3 \sinh(\xi b_3) + \cosh(\xi b_3)]B_3 + \cosh(\xi b_3)C_3 + [\xi b_3 \cosh(\xi b_3) + \sinh(\xi b_3)]D_3 = 0 \quad (3.91)$$

$$(1 - \lambda_3) \sinh(\xi b_3) A_3 + [(3 - \lambda_3) \cosh(\xi b_3) + (1 - \lambda_3) \xi b_3 \sinh(\xi b_3)] B_3 + (1 - \lambda_3) \cosh(\xi b_3) C_3 + [(3 - \lambda_3) \sinh(\xi b_3) + (1 - \lambda_3) \xi b_3 \cosh(\xi b_3)] D_3 = 0 \quad (3.92)$$

In order to obtain the contact pressure, we have to consider the surface, according to our coordinate system, $x_1 = 0$.

From the numerical procedure presented above in part 3.2.1, which is to match the displacements of the upper layer at a finite number of points on the contact surface, the normal displacement of layer 1 is needed:

$$\begin{aligned} u_1(x_1, y_1) &= \frac{1 - \nu_1^2}{\pi E_1} \int_0^{+\infty} \left[\frac{d^3 G_1}{dx_1^3} - \left(\frac{2 - \nu_1}{1 - \nu_1} \right) \xi^2 \frac{dG_1}{dx_1} \right] \cos(\xi y_1) \frac{d\xi}{\xi^2} \\ &= \frac{1 - \nu_1^2}{\pi E_1} \int_0^{+\infty} \left[(3B_1 + C_1) \xi^3 - \left(\frac{2 - \nu_1}{1 - \nu_1} \right) \xi^2 (B_1 + C_1) \xi \right] \cos(\xi y_1) \frac{d\xi}{\xi^2} \end{aligned} \quad (3.93)$$

Where

$$\begin{aligned} \frac{dG_1}{dx_1} &= (B_1 + C_1 + D_1 \xi x_1) \xi \cosh(\xi x_1) + (A_1 + D_1 + B_1 \xi x_1) \xi \sinh(\xi x_1) \\ &= (B_1 + C_1) \xi \end{aligned} \quad (3.94)$$

$$\begin{aligned} \frac{d^3 G_1}{dx_1^3} &= (3B_1 + C_1 + D_1 \xi x_1) \xi^3 \cosh(\xi x_1) + (A_1 + 3D_1 + B_1 \xi x_1) \xi^3 \sinh(\xi x_1) \\ &= (3B_1 + C_1) \xi^3 \end{aligned} \quad (3.95)$$

Utilize the relationship (3.82):

$$B_1 + C_1 = 0$$

Finally, we obtain

$$u_1(x_1, y_1) = \frac{1 - \nu_1^2}{\pi E_1} \int_0^{+\infty} 2B_1 \cos(\xi y_1) \xi d\xi \quad (3.96)$$

Where B_1 is related with properties of all the layers, such as Young's modulus, Poisson's ratios and thicknesses.

From the normal displacement expression (3.96) and (2.31), we can see, for the contact problems of the single-layered and multi-layered solids, even though the kernels are different for them, the basic numerical solution procedures are same.

When a layer is put into an elastic solid, it will definitely affect the pressure distribution and the stress-strain fields. The schematic presentations of the contact problems are shown in Figure 3.4 and Figure 3.14. First, for a solid without a middle layer, it has Young's modulus $E_1=1.06E7$ psi and Poisson's ratio $\nu_1 = 0.3$, thickness $b_1=21a$. When the rigid punches are pushed into the elastic solid, contact pressure can be obtained by the numerical procedure. Then, middle layers are put into the elastic solid. Usually a stiffer middle layer will increase the contact pressure; a softer middle layer will decrease the contact pressure. Figure 3.15 illustrates the effect of middle layers on the contact pressure, which gives us the basic introductions to the role of middle layers. Later detailed research about the effect of middle layer thickness on contact pressure will be presented. Meanwhile, the influence of Young's modulus and Poisson's ratio of middle layers on contact pressure will also be shown.

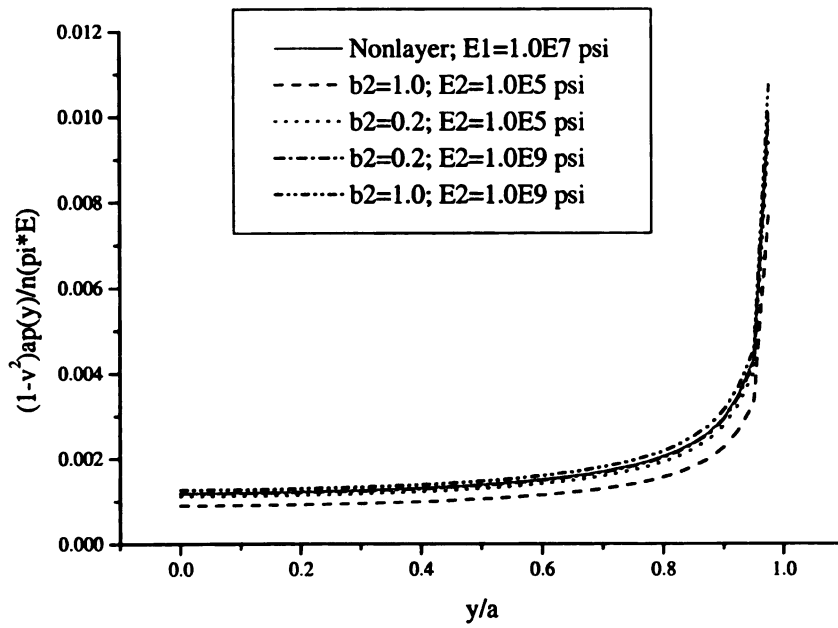


Figure 3.15 Comparison of contact pressures between non-middle layer and thin middle layer

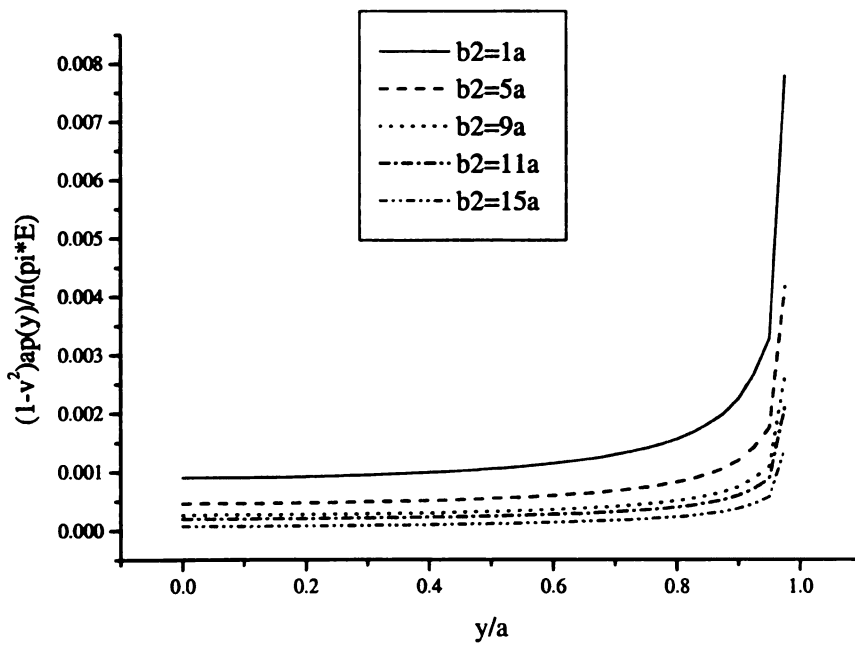


Figure 3.16 Influence of various layer thicknesses on contact pressure

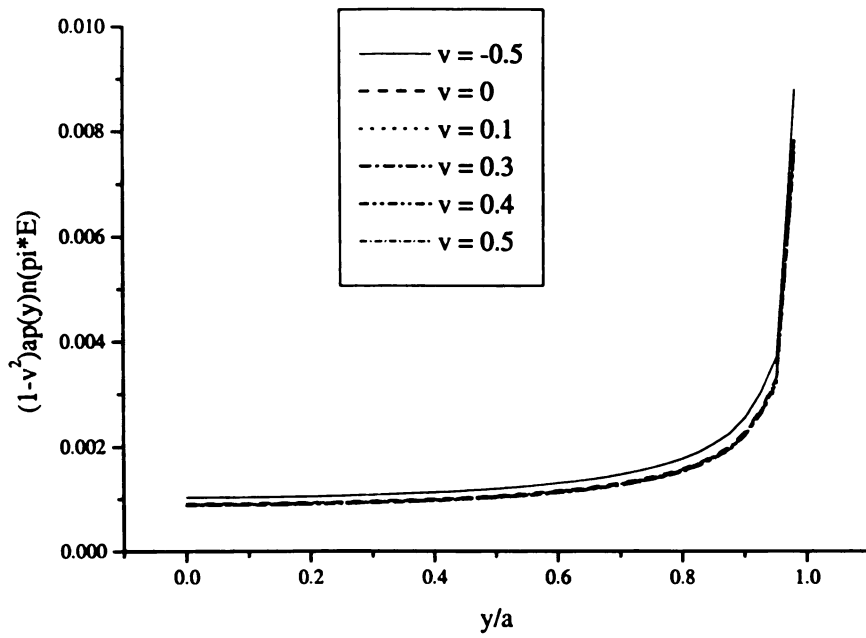


Figure 3.17 Influence of Poisson's ratios on contact pressure

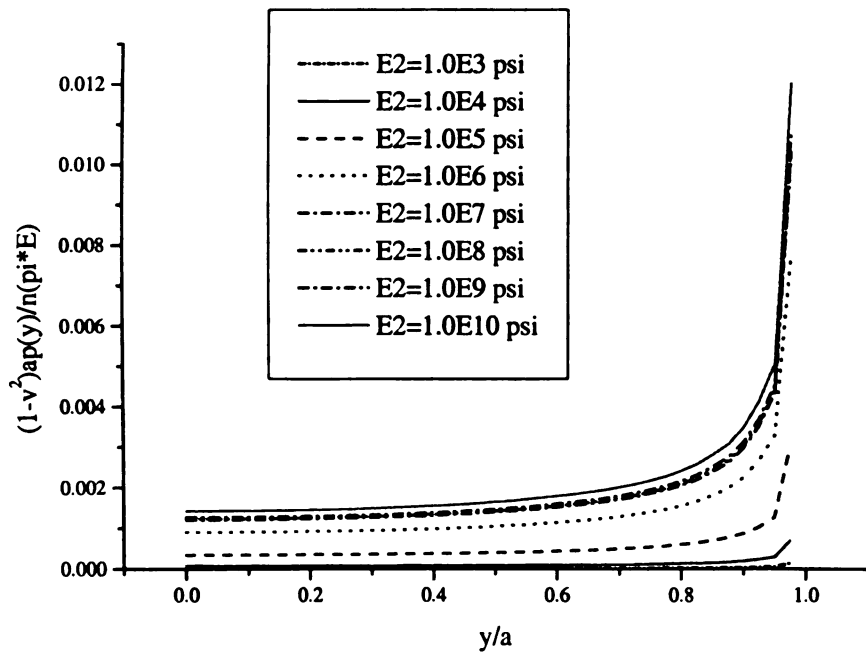


Figure 3.18 Effect of Young's moduli of middle layers on contact pressure

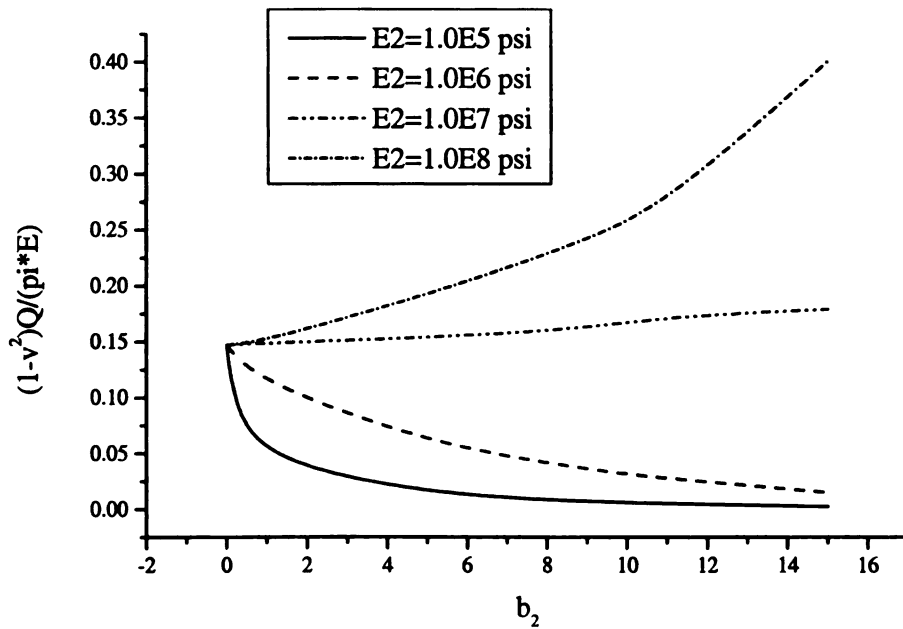


Figure 3.19 Total loads versus middle layer thicknesses

| | 1.0E5 | 1.0E6 | 1.0E7 | 1.0E8 |
|-----|---------|---------|---------|---------|
| 0 | 0.14688 | 0.14688 | 0.14688 | 0.14688 |
| 0.2 | 0.09026 | 0.13781 | 0.14757 | 0.14754 |
| 1 | 0.04284 | 0.11196 | 0.14848 | 0.15137 |
| 5 | 0.01327 | 0.05864 | 0.15335 | 0.19131 |
| 9 | 0.00697 | 0.03559 | 0.16199 | 0.24035 |
| 11 | 0.00516 | 0.02761 | 0.17239 | 0.27361 |
| 15 | 0.00261 | 0.01492 | 0.17906 | 0.40058 |

Table 3.1 Numerical solutions of total loads for different thicknesses and Young's moduli of middle layers

A change in the thickness of the middle layer makes an appreciable effect on the contact pressure. For the softer layers, they will decrease the contact pressure. The magnitude of effect of layer thickness on contact pressure depends on the ratio of the middle layer thickness and the total thickness of the solid. The bigger the ratio, the more will the

contact pressure be decreased. Figure 3.16 presents the results of a solid with a special total thickness $b = 21a$ pressed by rigid flat punches. The contact problem is shown schematically in Figure 3.14, $E_1 = E_3 = 10.6E6$ psi, $E_2 = 10E5$ psi; $\nu_1 = \nu_3 = 0.3$, $\nu_2 = 0.49$; $b_1 = b_3$. As the layer thickness increases and the total thickness keeps the same, the ratio of thickness of middle layer to total solid becomes bigger. Consequently the contact pressure turns less. If a stiffer middle layer is put into the solid, the contrary trend will be expected.

The Poisson's ratio can be seen to have little effect on the change of contact pressure for the special ratio of middle layer thickness to total solid thickness. The maximum possible change for the positive Poisson's ratio, from $\nu = 0.5$ to $\nu = 0$, produces a 0.69 percentage increase in contact pressure at the middle point of the contact zone. Even we consider the negative Poisson's ratios, though they are not so common for the practical medium, the influence of the Poisson's ratio is still not so much. Only 10 percentage increase in contact pressure can be seen for the exhausted change from $\nu = 0.5$ to $\nu = -0.5$. This effect can be seen clearly in Figure 3.17.

Compared with that of the Poisson's ratio, the effect of the Young's modulus E_2 of middle layers on the contact pressure is quite considerable. When a layer with a smaller Young's modulus is put into the elastic solid, the contact pressure of the contact region is very greatly decreased. Depending on the material properties and geometry, contact pressure can drop into a very low level. Which is probably one of the reasons that the layered solids become popular. On the contrary, a stiffer middle layer can raise the

contact pressure evidently. But the magnitude of the increase in contact pressure because of the stiffer middle layer addition is not so obvious as that of the decrease in contact pressure because of the softer middle layer addition. For example, for the same ratio of middle layer thickness to total solid thickness and same Poisson's ratio, with regard to the Young's modulus change of middle layers from $E_2 = 1.0E5$ psi to $E_2 = 1.0E3$ psi, a 65 percentage decrease in contact pressure at the middle point of the contact zone can be seen. However, for the Young's modulus change of middle layers from $E_2 = 1.0E7$ psi to $E_2 = 1.0E10$ psi, only 18 percentage increase in contact pressure at the middle point of the contact area can be expected. Figure 3.18 illustrates the trend in detail, in which the line of $E_2=1.0E6$ psi is for the contact problem of a single-layered solid pressed by symmetrical flat punches.

Figure 3.19 shows the effect of the middle layer thickness and Young's modulus on total load that we need in order to obtain the same indentation depth. The line of $E_2 = 1.0E7$ psi has the same Young's modulus for the whole solid. However, the Poisson's ratio of middle layer is 0.49 which is different from that of the solid $\nu_1 = 0.3$. The plot is almost a straight line with a slope of zero. Which verifies the small effect of Poisson's ratio on the contact problems for the special thickness ratio that we concluded above again. From the graph, we can see a contrary trend for stiffer and softer middle layer as the increase of its thickness. Meanwhile we can also easily figure out the total loads we need for different thicknesses of the middle layers to obtain the special indentation depth. Numerical solutions of total loads in accordance with different middle layer thicknesses and Young's moduli are presented in Table 3.1 for practical uses.

3. 3 Non-conforming Contact Problem

For this kind of contact problems, because both of the contact length a and the contact pressure distribution $p(y)$ are unknown, the exact solution is not available, except very special cases, for example, infinite domain. Therefore, we need use the numerical solution procedure to solve this kind of problems. By taking rigid cylinders as indenters, the detailed solution procedure and main results are presented in the following. Considering the discussion about the conforming contact problem mentioned before, we can subdivide the problem into two cases: two symmetrical rigid cylinders on a single-layered elastic solid and two symmetrical rigid cylinders on a multi-layered elastic solid.

3. 3. 1 Rigid Cylinders on a Single-layered Elastic Solid

Figure 3.20 illustrates the contact problem of an elastic solid of thickness $2b$ compressed between two same rigid cylinders. If we assume the cylindrical indenters have circular surface of radius R and long enough along z -axis, the contour of the circular surface is known and we can treat this problem as plane strain problem. Because the indenters are rigid and frictionless, the normal displacement u of the elastic solid that is pressed, according to the coordinates shown in Figure 3.20, can be

On $x = \pm b$:

$$u = \pm b \mp [\delta - (R - \sqrt{R^2 - y^2})] \quad |y| \leq a \quad (3.97)$$

Where

δ : indentation depth

a: half contact length

b: thickness of a half of the solid

R: radius of the rigid cylinder

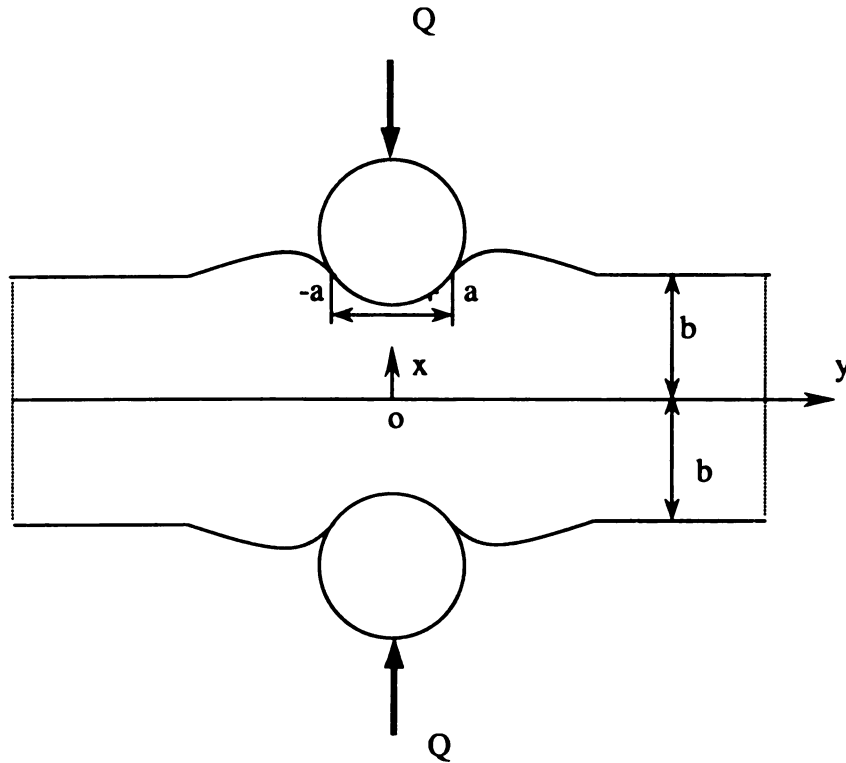


Figure 3.20 rigid cylinders on a single-layered elastic solid

Introducing dimensionless variables $s = \frac{x}{b}$, $\beta = \frac{y}{b}$, and $\omega = \xi b$, the expressions of

constant A and D can be summarized as

$$A = \frac{2[\sinh \omega + \omega \cosh(\omega)]}{2\omega + \sinh(2\omega)} \frac{b^2}{\omega^2} \frac{\sin\left(\omega \frac{a}{b}\right)}{\omega \frac{a}{b}} \quad (3.98)$$

$$D = -\frac{4 \sinh(\omega)}{2\omega + \sinh(2\omega)} \frac{b^2}{\omega^2} \frac{\sin\left(\omega \frac{a}{b}\right)}{\omega \frac{a}{b}} \quad (3.99)$$

Define a function $\bar{G}(s, \omega)$ as

$$\bar{G}(s, \omega) = \frac{1}{b^2} G(s, \omega) = \frac{1}{b^2} [A \cosh(\omega s) + D(\omega s) \sinh(\omega s)] \quad (3.100)$$

Where A and D are given by equation (3.98) and (3.99)

The expression of normal displacement of the surface is rewritten as

$$u(s, \beta) = \frac{1-\nu^2}{\pi E} \int_0^{+\infty} \left[\frac{d^3 \bar{G}}{ds^3} - \left(\frac{2-\nu}{1-\nu} \right) \omega^2 \frac{d\bar{G}}{ds} \right] \cos(\omega \beta) \frac{d\omega}{\omega^2} \quad (3.101)$$

On the surface, normal displacement can be denoted in terms of the function $K(\beta)$ as follows

$$\bar{u}(\beta) = \frac{1-\nu^2}{\pi E} K(\beta) \quad (3.102)$$

Where

$$K(\beta) = \int_0^{+\infty} \left[\frac{d^3 \bar{G}}{ds^3} - \left(\frac{2-\nu}{1-\nu} \right) \omega^2 \frac{d\bar{G}}{ds} \right] \cos(\omega \beta) \frac{d\omega}{\omega^2} \quad (3.103)$$

It is also convenient to introduce a coordinate value ε relative to the half contact length and to define the function $\bar{K}(\varepsilon)$ as

$$\bar{K}(\varepsilon) = K\left(\frac{a}{b} \varepsilon\right) \quad (3.104)$$

$$\varepsilon = \frac{y}{a} \quad (3.105)$$

So the total contact zone is $-1 \leq \varepsilon \leq +1$.

In the contact area, if the contact pressure distribution is an arbitrary function $p(\varepsilon)$, then we know the normal displacement for the arbitrary contact pressure $p(\varepsilon)$ is

$$\frac{1-\nu^2}{\pi E} a \int_{-1}^{+1} p(\eta) \bar{K}(|\varepsilon - \eta|) d\eta = u(\varepsilon) \quad (3.106)$$

We can rewrite the equation (3.106) as

$$\frac{1-\nu^2}{\pi E} a \left\{ \int_0^{+1} p(\eta) [\bar{K}(|\varepsilon - \eta|) + \bar{K}(|\varepsilon + \eta|)] d\eta \right\} = u(\varepsilon) \quad (3.107)$$

Define

$$\bar{Q}(\varphi, \eta) = \bar{K}(|\varphi - \eta|) + \bar{K}(|\varphi + \eta|) \quad (3.108)$$

We have

$$\frac{(1-\nu^2)}{\pi E} a \int_0^{+1} \bar{Q}(\varepsilon, \eta) p(\eta) d\eta = u(\varepsilon) \quad (3.109)$$

We know there is an extra unknown item: contact length $2a$, comparing with the conforming contact problem. Which is the main difference between these two kinds of contact problems. So some modifications need to be made in order to use the numerical solution procedure to solve the kind of contact problems.

Looking at the boundary condition (3.97), we have

$$u(y) - u(a) = \sqrt{R^2 - a^2} - \sqrt{R^2 - y^2} \quad |y| \leq a \quad (3.110)$$

Utilizing the coordinate value ε , the boundary condition can be rewritten as

$$u(\varepsilon) - u(1) = a \left[\sqrt{\left(\frac{R}{a}\right)^2 - 1} - \sqrt{\left(\frac{R}{a}\right)^2 - \varepsilon^2} \right] \quad |\varepsilon| \leq 1 \quad (3.111)$$

According to the normal displacement equation (3.109), we know

$$\frac{(1-\nu^2)}{\pi E} \int_0^1 [\bar{Q}(\varepsilon, \eta) - \bar{Q}(1, \eta)] p(\eta) d\eta = \left[\sqrt{\left(\frac{R}{a}\right)^2 - 1} - \sqrt{\left(\frac{R}{a}\right)^2 - \varepsilon^2} \right] \quad (3.112)$$

Further

$$\frac{(1-\nu^2)}{\pi E} \int_0^1 W(\varepsilon, \eta) p(\eta) d\eta = \left[\sqrt{\left(\frac{R}{a}\right)^2 - 1} - \sqrt{\left(\frac{R}{a}\right)^2 - \varepsilon^2} \right] \quad (3.113)$$

Where

$$W(\varepsilon, \eta) = [\bar{Q}(\varepsilon, \eta) - \bar{Q}(1, \eta)] \quad (3.114)$$

So the numerical solution procedure can be modified as

$$\frac{(1-\nu^2)}{\pi E} \sum_{i=1}^n W(\varepsilon_j, \eta_i) p(\eta_i) = \left[\sqrt{\left(\frac{R}{a}\right)^2 - 1} - \sqrt{\left(\frac{R}{a}\right)^2 - \varepsilon_j^2} \right] \quad j=1, n \quad (3.115)$$

Where

$$\begin{aligned} W(\varepsilon_j, \eta_i) &= \bar{Q}(\varepsilon_j, \eta_i) - \bar{Q}(1, \eta_i) \\ &= \bar{K}(|\varepsilon_j - \eta_i|) + \bar{K}(|\varepsilon_j + \eta_i|) - \bar{K}(|1 - \eta_i|) - \bar{K}(|1 + \eta_i|) \end{aligned} \quad (3.116)$$

In this way, we can make the problem solvable by the numerical procedure. By solving the matrix equation, the distribution of the contact pressure can be obtained.

$$\frac{(1-\nu^2)}{\pi E} \begin{bmatrix} W_{11} & W_{12} & \cdots & W_{1n-1} & W_{1n} \\ W_{21} & W_{22} & \cdots & W_{2n-1} & W_{2n} \\ \vdots & \vdots & \ddots & \vdots & \vdots \\ W_{n-11} & W_{n-12} & \cdots & W_{n-1n-1} & W_{n-1n} \\ W_{n1} & W_{n2} & \cdots & W_{nn-1} & W_{nn} \end{bmatrix} \begin{Bmatrix} p_1 \\ p_2 \\ \vdots \\ p_{n-1} \\ p_n \end{Bmatrix} = \begin{bmatrix} \sqrt{H^2 - 1} - \sqrt{H^2 - \varepsilon_1^2} \\ \sqrt{H^2 - 1} - \sqrt{H^2 - \varepsilon_2^2} \\ \vdots \\ \sqrt{H^2 - 1} - \sqrt{H^2 - \varepsilon_{n-1}^2} \\ \sqrt{H^2 - 1} - \sqrt{H^2 - \varepsilon_n^2} \end{bmatrix} \quad (3.117)$$

$$H = \frac{R}{a} \quad (3.118)$$

First, the confirmation of efficiency and validity of the numerical procedure for the non-conforming contact problems needs to be preformed. As mentioned in part 3.2.1, we introduce a contact problem between a rigid cylinder and a half-space medium. We will have the same form of function $G(x, \xi)$ (3.31), and we have the same boundary conditions as (3.25), (3.26) and (3.28). But since it is a cylindrical punch, we have a different normal displacement condition:

On $x = 0$:

$$u(y) = \delta - \left(R - \sqrt{R^2 - y^2} \right) \quad (3.119)$$

Using the numerical procedure presented above, we can obtain numerical solution of the distribution of the contact pressure. Figure 3.21 illustrates a comparison between numerical solution and exact solution [28] of contact problem by a rigid cylinder on an elastic half space. The plots show clearly the effects of different simulation point numbers on the distribution of the contact pressure. When we choose 40 or 50 points, the results are very close to the exact solution. So the numerical procedure is also applicable for non-conforming contact problem. Figure 3.22 presents the comparison of contact pressure simulations of 40 points and 50 points in the half contact area. The solutions are very close. So we can use 40 points to simulate the distribution of contact pressure in half contact length, which saves about 25% computation time.

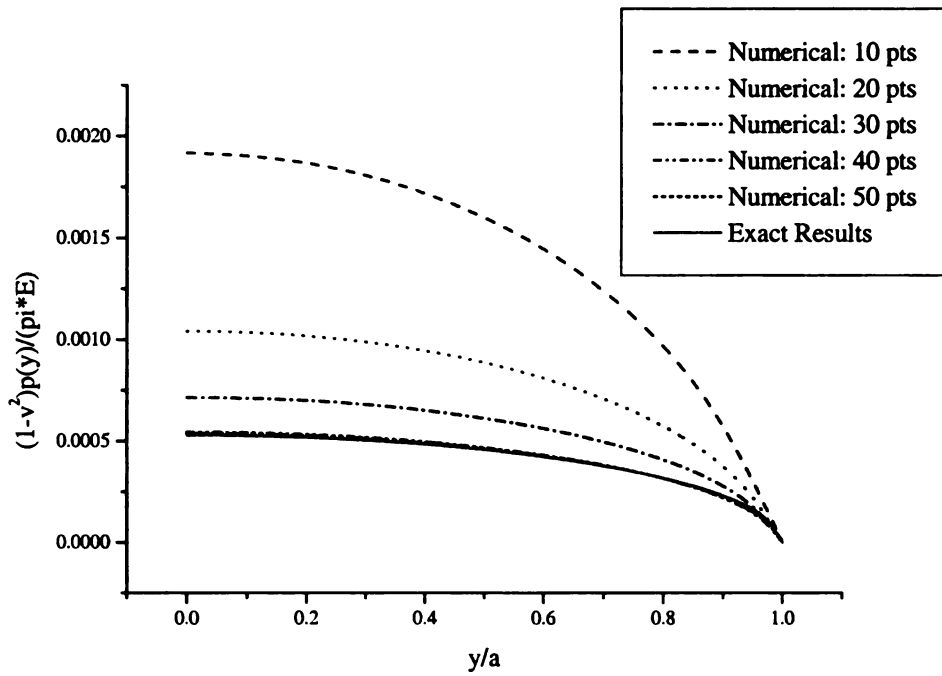


Figure 3.21 Comparison between numerical solution and exact solution of contact problem by a rigid cylinder on a half space

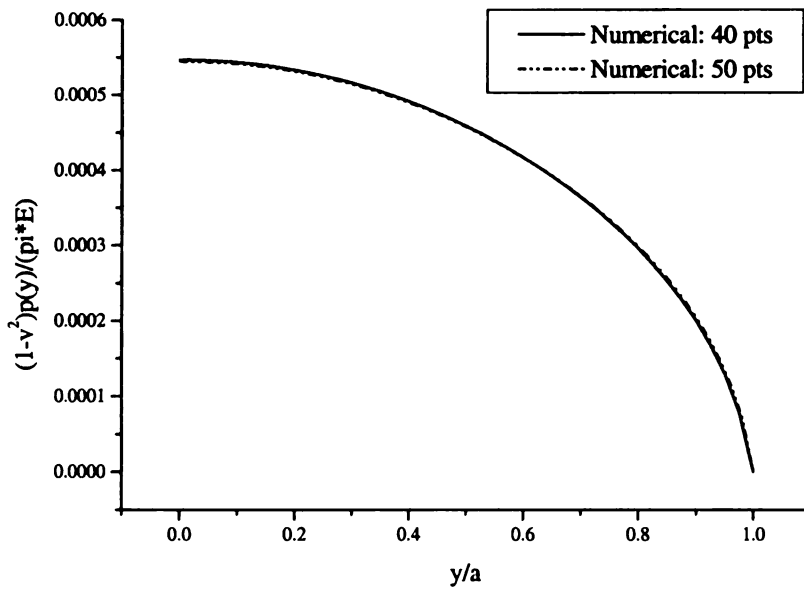


Figure 3.22 Comparison of results between 40 points and 50 points

Comparing with the conforming contact problems, non-conforming contact problems have maximum contact pressure at the middle point of the contact zone, and decrease to zero at the end of the contact area. While conforming contact problems have minimum contact pressure at the middle point of the contact region, and infinity at the end of the contact area.

With regard to the single-layered elastic solid, thickness of the solid has different effects on the contact pressure distribution $p(y)$, depending on the ratio of contact length to total thickness of the elastic solid. The ratio of radius of the cylinder: R and the half contact length: a is fixed. The distributions of contact pressure corresponding to the change of ratio of half contact length: a and solid thickness: b are shown in Figure 3.23. Which tells us that change of the thickness has very little effect on contact pressure when the elastic solid is thick and the ratio of cylinder radius to half contact length is fixed at 10. However, when it is thin, change of the thickness has a very considerable effect on the distribution of the contact pressure. In order to study the effect of the ratio of cylinder radius to half contact length in the procedure, we adjust the ratio to 2. The very similar trend is illustrated in Figure 3.24, even though the contact pressures are increased into much higher levels.

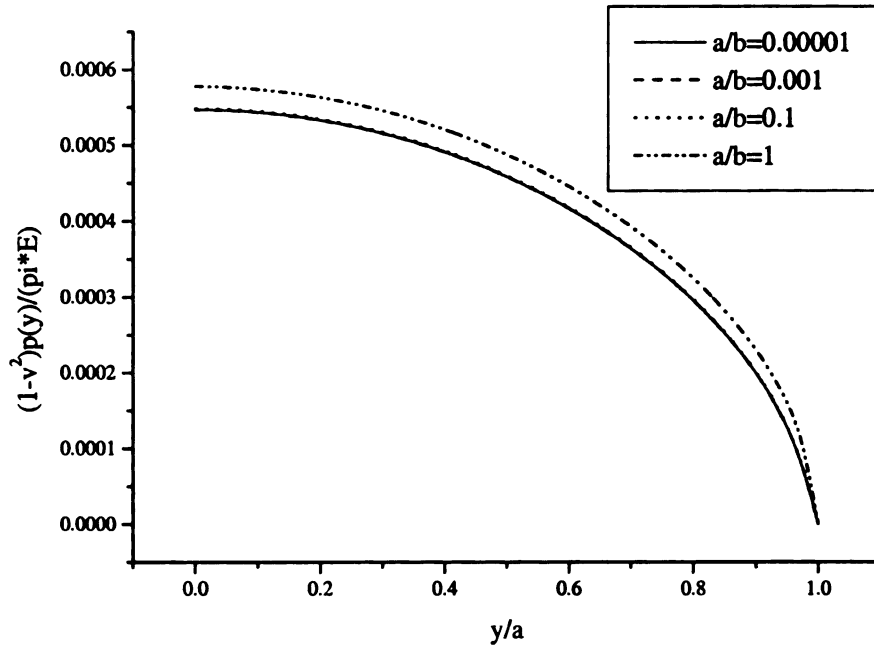


Figure 3.23 Contact pressure distribution for various a/b , $R/a=10$

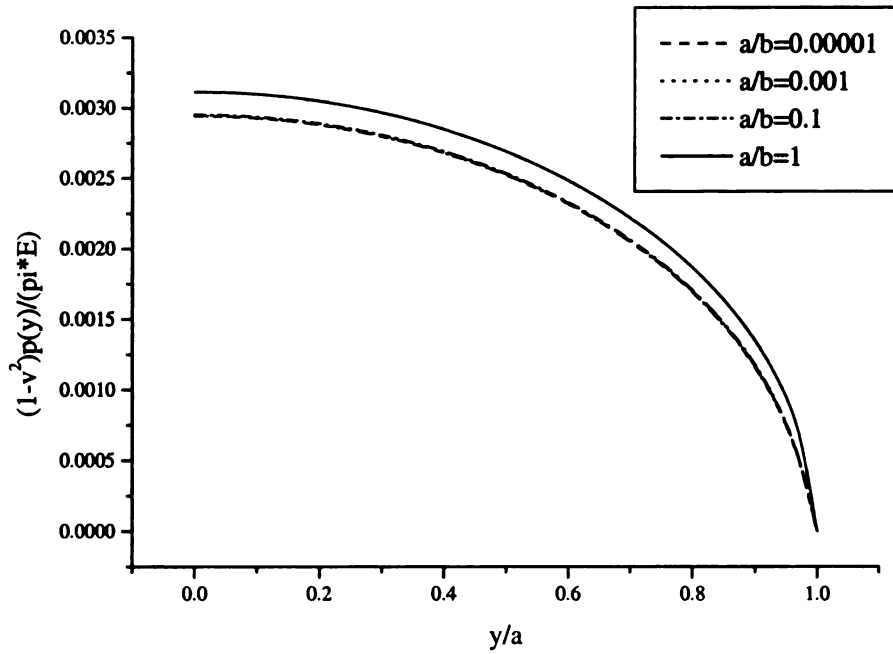


Figure 3.24 Contact pressure distribution for various a/b , $R/a=2$

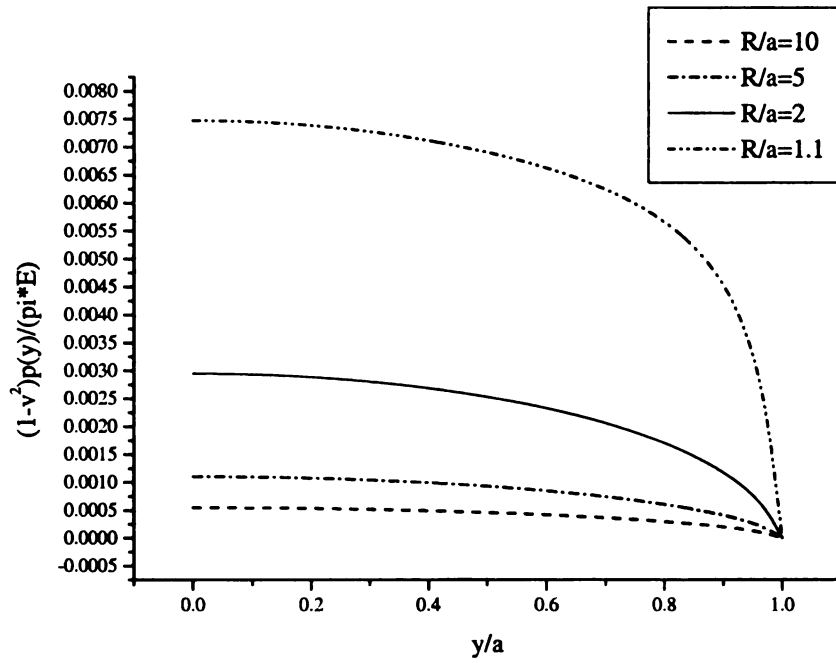


Figure 3.25 Contact pressure distribution for various R/a , $a/b=0.1$

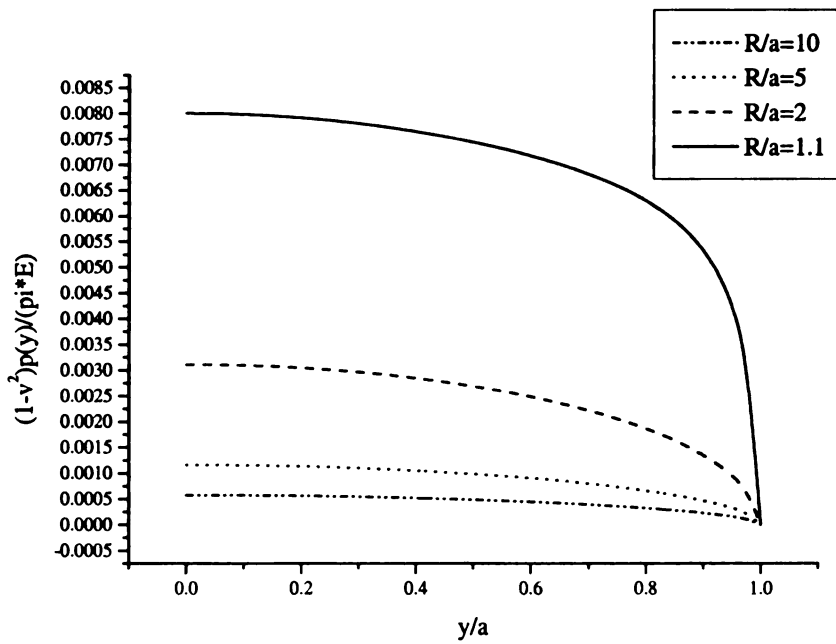


Figure 3.26 Contact pressure distribution for various R/a , $a/b=1$

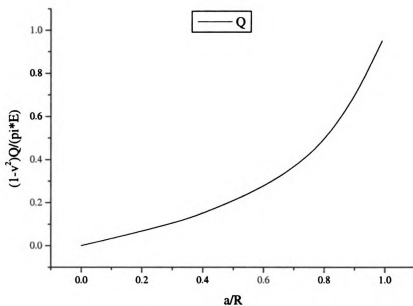


Figure 3.27 Total loads versus half contact lengths

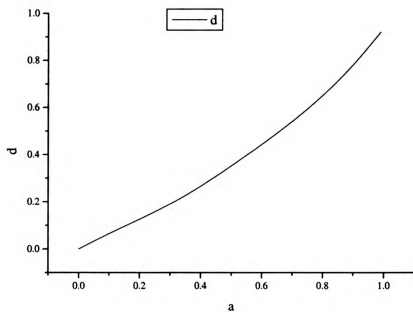


Figure 3.28 Relationship between half contact length and indentation depth

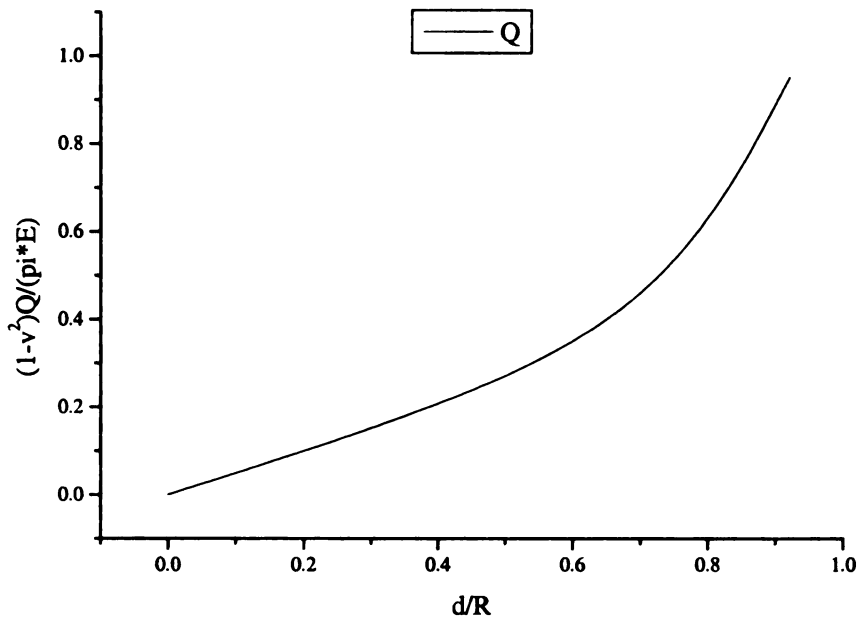


Figure 3.29 Total loads versus indentation depths

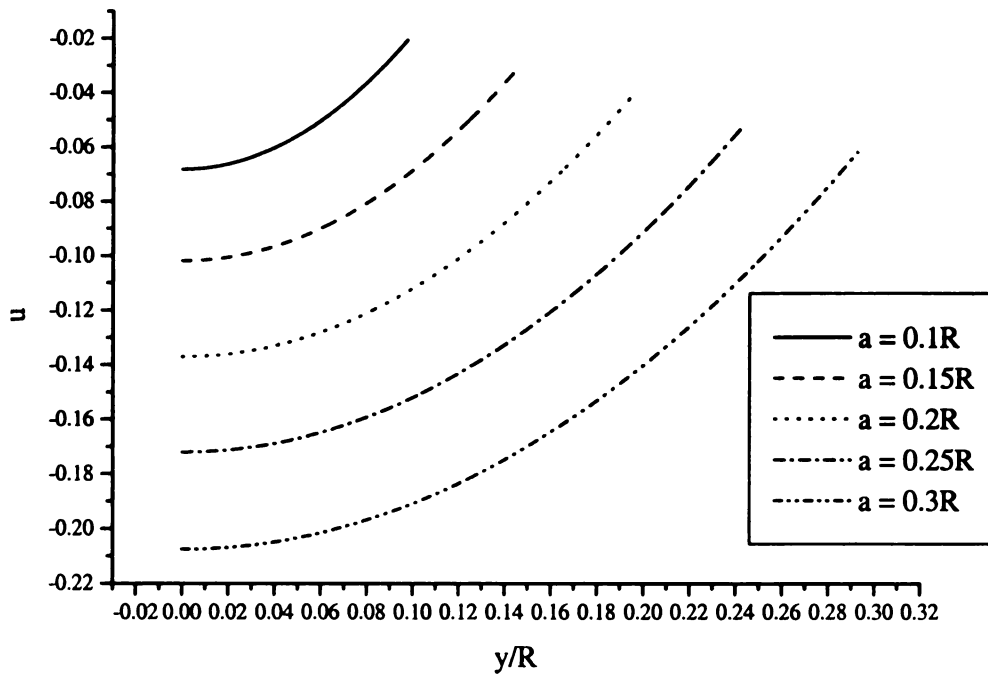


Figure 3.30 Normal displacements in the contact area

Figure 3.25 shows the huge effects of the ratio of cylinder radius to half contact length on the distribution of contact pressure. When the ratio is really big, the increase of contact pressure is almost linear. As the half contact length is close to the radius of the cylinder, the contact pressure increases greatly. For example, from the radius $R/a = 2$ to $R/a = 1.1$, a 150% increment of contact pressure at the middle point of the contact area is shown. The phenomena can be seen more clearly in Figure 3.27, which gives the relationship between total loads and half contact lengths. We can see when $R \gg a$, the relationship between total load and half contact length is almost linear. As half contact length increases, the relationship turns nonlinear. In Figure 3.26, the ratio of half contact length and solid thickness a/b is changed. A similar trend as that shown in Figure 3.25 is presented. When R is fixed, increasing a/b means the solid is thinner. Referring to Figure 3.25 and Figure 3.26, we can conclude that the effect of the thickness change is negligible comparing with that of contact length change. The relationship between half contact lengths and indentation depths is shown in Figure 3.28. It is clear that it is nonlinear when a/R can not be treated as very small values. Figure 3.29 further gives the relationship between total loads and indentation depths. From which we can easily figure out total load or indentation depth by giving any one between them. Some examples of normal displacements in the contact area, $a/R=0.1$, $a/R=0.15$, $a/R=0.2$, $a/R=0.25$, and $a/R=0.3$, are presented in Figure 3.30.

3. 3. 2 Rigid Cylinders on a Multi-layered Elastic Solid

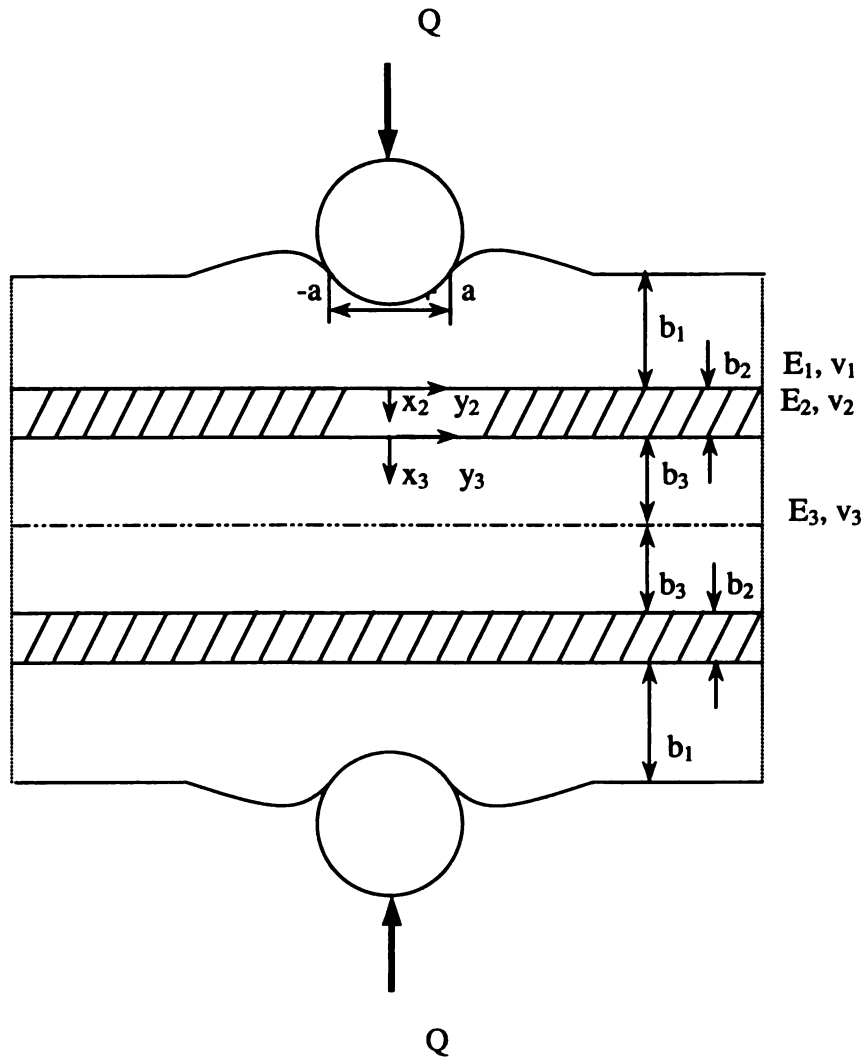


Figure 3.31 rigid cylinders on a multi-layered elastic solid

Because of the importance and practical uses of the contact problems of layered elastic solids in science and engineering, the effects of the properties of layers on the contact pressure distribution need to be investigated. Figure 3.31 presents schematically a multi-layered elastic solid pressed by two symmetrical rigid cylinders. Perfect adherence between layers is assumed, and the cylinders are supposed to be frictionless. In order to

concentrate our attention on the influence of the middle layers, we make layer 1 and layer 3 have same properties, such as thicknesses, Young's modulus, and Poisson's ratio, but they can be different if required.

The coordinate systems are shown in Figure 3.31, where subscript 1 is used to stand for layer 1, subscript 2 for layer 2, and so on. The boundary conditions are given by equations (3.55) ~ (3.59). Because the indenters are frictionless rigid cylinders, according to the coordinate systems, we have

On $x_1 = 0$:

$$u_1(y_1) = \delta - (R - \sqrt{R^2 - y_1^2}) \quad |y_1| \leq a \quad (3.120)$$

Where

δ : indentation depth

a : half contact length

R : radius of the rigid cylinder

Due to the different coordinate systems, the extra boundary condition for this contact problem is different from equation (3.110)

$$u(y) - u(a) = \sqrt{R^2 - y^2} - \sqrt{R^2 - a^2} \quad |y| \leq a \quad (3.121)$$

For this symmetrical contact problem presented in Figure 3.31, to obtain the general Airy stress functions, we need utilize boundary conditions to determine 12 constants. Following the same derivation as part 3.2.4, we obtain the final normal displacement

expression (3.96). Then using the numerical procedure, a matrix equation can be formulated to compute the contact pressure.

$$\frac{(1-\nu^2)}{\pi E} \begin{bmatrix} \bar{W}_{11} & \bar{W}_{12} & \cdots & \bar{W}_{1n-1} & \bar{W}_{1n} \\ \bar{W}_{21} & \bar{W}_{22} & \cdots & \bar{W}_{2n-1} & \bar{W}_{2n} \\ \vdots & \vdots & \ddots & \vdots & \vdots \\ \bar{W}_{n-11} & \bar{W}_{n-12} & \cdots & \bar{W}_{n-1n-1} & \bar{W}_{n-1n} \\ \bar{W}_{n1} & \bar{W}_{n2} & \cdots & \bar{W}_{nn-1} & \bar{W}_{nn} \end{bmatrix} \begin{Bmatrix} p_1 \\ p_2 \\ \vdots \\ p_{n-1} \\ p_n \end{Bmatrix} = \begin{bmatrix} \sqrt{H^2 - \varepsilon_1^2} - \sqrt{H^2 - 1} \\ \sqrt{H^2 - \varepsilon_2^2} - \sqrt{H^2 - 1} \\ \vdots \\ \sqrt{H^2 - \varepsilon_{n-1}^2} - \sqrt{H^2 - 1} \\ \sqrt{H^2 - \varepsilon_n^2} - \sqrt{H^2 - 1} \end{bmatrix} \quad (3.122)$$

In engineering, putting a middle layer into an elastic solid can affect the distribution of contact pressure. Depending on different properties of middle layers, they have different levels of effects. These effects about rigid flat punches have been investigated in the preceding parts. The following presents the effects of middle layers on the contact pressure distribution in accordance with rigid cylindrical indenters.

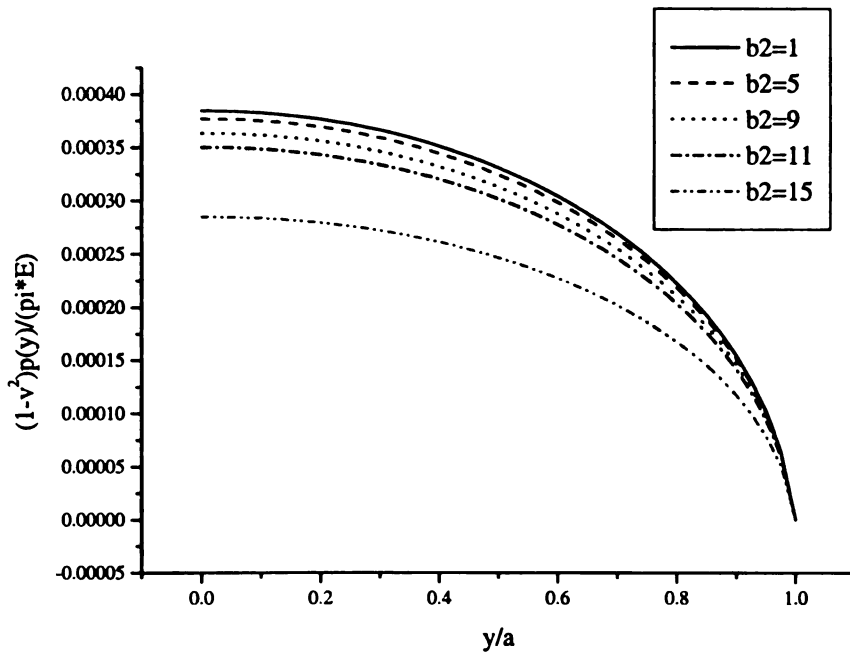


Figure 3.32 Layer thickness' effect on contact pressure distribution

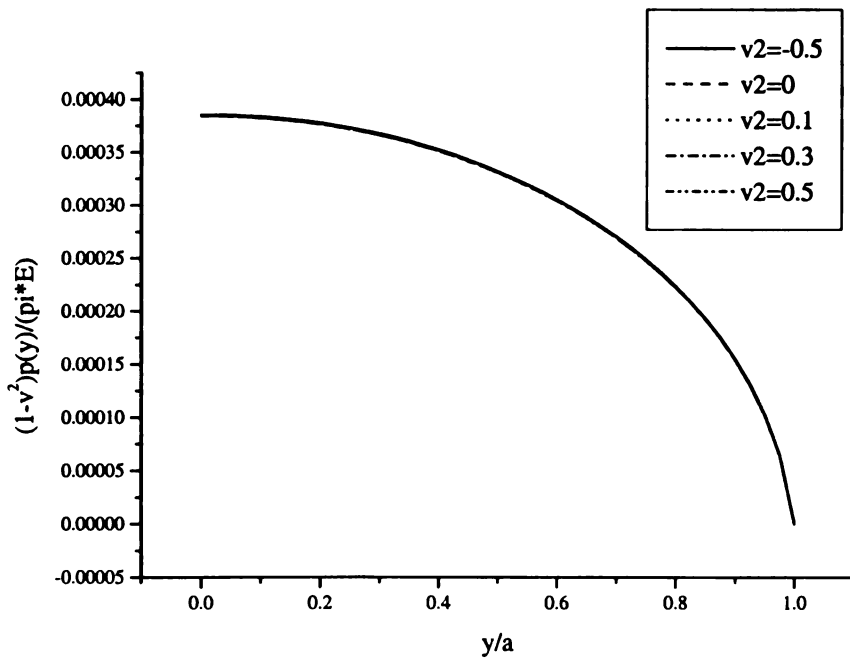


Figure 3.33 Poisson's ratio's effect on contact pressure distribution

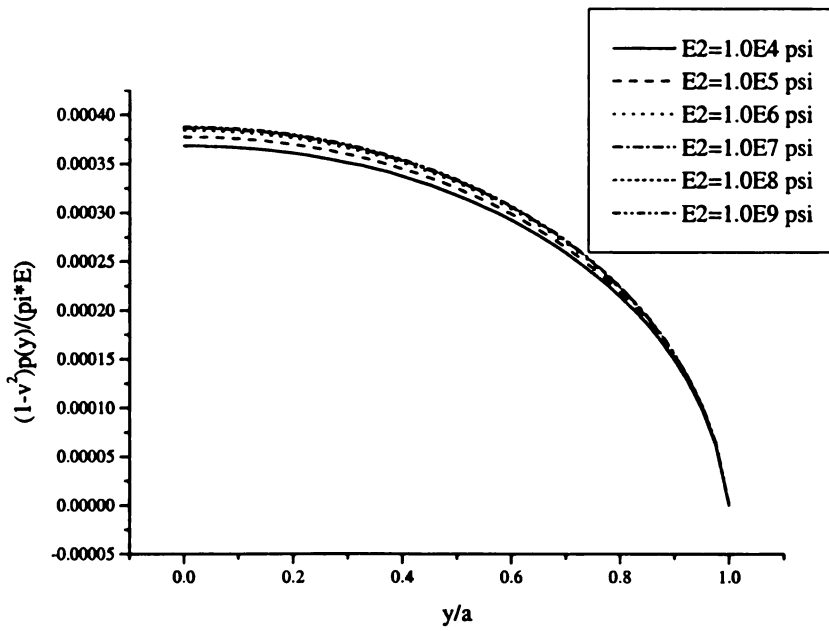


Figure 3.34 Young's modulus' effect on contact pressure distribution

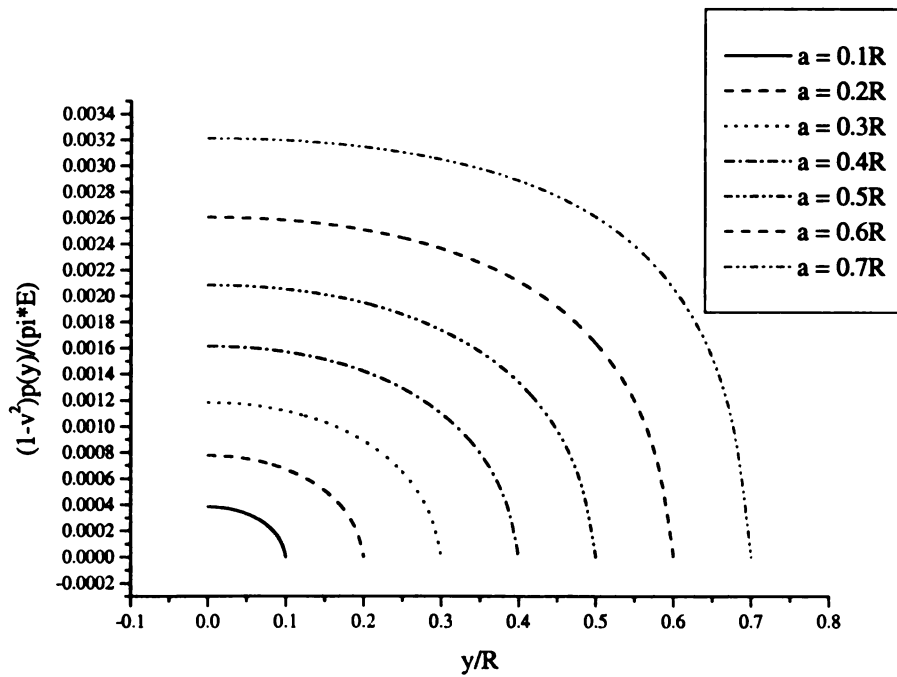


Figure 3.35 Contact pressure variations for various half contact lengths

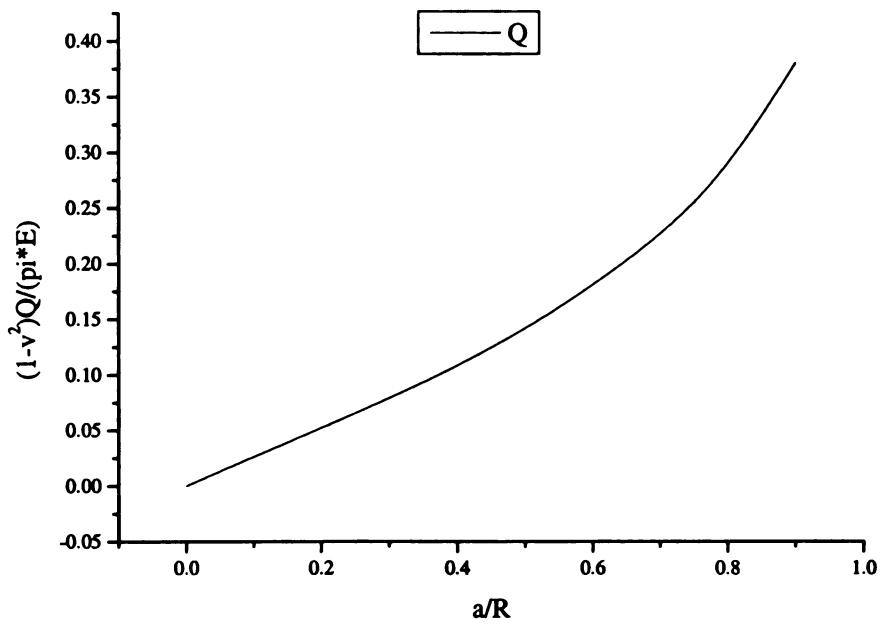


Figure 3.36 Total loads for different half contact lengths.

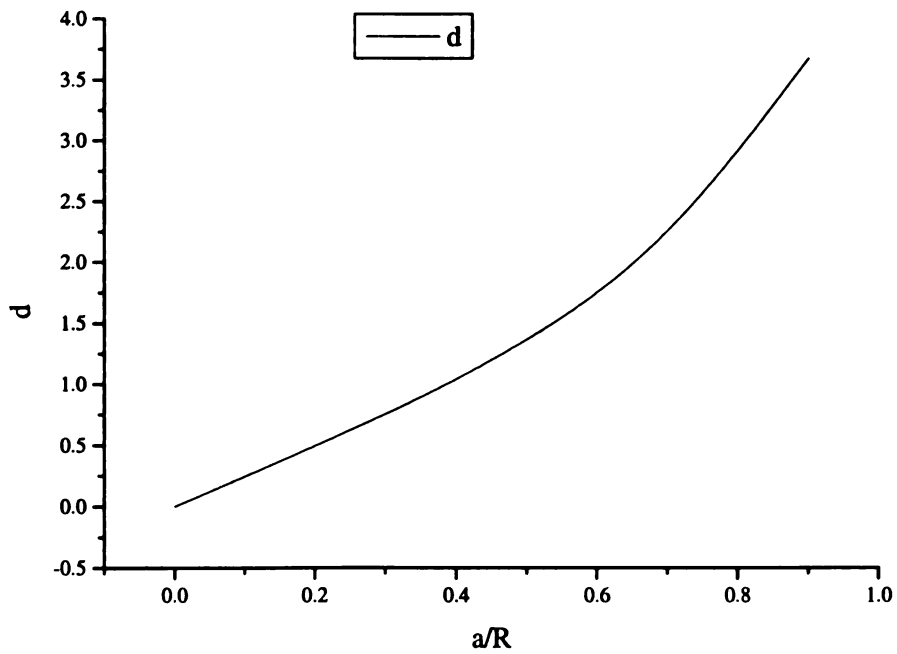


Figure 3.37 Half contact lengths versus indentation depths

Figure 3.32 shows the influence of the middle layer thickness on contact pressure when the middle layers are softer than the elastic solid. As the thicknesses of the middle layers increase, the contact pressure turns smaller and smaller. Depending on different properties of middle layers, the contact pressure can decrease into a very low level.

Figure 3.33 depicts the little effect of Poisson's ratio on the distribution of contact pressure. For the contact problem shown in Figure 3.31, where $E_1=E_3=1.0E7$ psi, $E_2=1.0E6$ psi; $b_1=b_3=10$, $b_2=1$; $\nu_1=\nu_3=0.3$. The Poisson's ratio of the middle layer ν_2 changes from -0.5 to 0.5 , while the numerical solutions of the contact pressures are very similar for the different Poisson's ratios. They are so close that the effects of changing Poisson's ratio of middle layers on contact pressure for this case can be negligible.

Figure 3.34 tells the effect of the Young's modulus of the middle layer on the distribution of the contact pressure for the special domain. Though changing E_2 affects contact pressure distribution, the influence is very little.

Changing contact length has direct impact on the distribution of contact pressure. Figure 3.35 shows the big effects. From the plots, we can easily find the contact pressure according to the contact length. Figure 3.36 further illustrates the relationship between total loads and half contact lengths. The nonlinear relationship between half contact lengths and indentation depths is presented in Figure 3.37.

Chapter 4

CONCLUSIONS AND FUTURE WORK

4. 1 Conclusions

Contact in mechanics of solids and structures has a very fundamental role. But because of its difficulty and complexity, contact problem has been providing a challenge to mathematicians and engineers since the 1880's. During recent years, because of the wide application of layered solids in highly technological areas, the contact problem of layered solids has aroused general concern and interest in many areas of engineering.

In the work, contact problems of an elastic layered solid indented by rigid punches are solved by using Fourier Transforms. The contact problems are divided into two cases: conforming contact problem and non-conforming contact problem, according to the different rigid punches. In order to obtain the distribution of the contact pressure, numerical procedures are introduced separately for the different contact problems. Two kernels, rectangular one and triangular one, are used and compared each other to increase the efficiency and accuracy of computation. The rectangular kernel is chosen finally. Comparisons of numerical results and exact analytical solutions of the half-space contact problem are made to confirm the validity of the numerical solution procedures separately. Satisfactory results of comparisons are obtained. Then the method is extended to the static problems about the contact of the rigid punches on a multi-layered elastic solid.

During the work, both conforming contacts and non-conforming contact are investigated in detail.

In reality, the distribution of the contact pressure is considerably different from the classical case. For example, when the thickness of the elastic solid is not infinite, the result for this contact problem has big difference from the classical solution of the infinite domain. Numerical results for the contact problems of the finite domain are presented to illustrate the difference in the work. The relationships between total loads and indentation depths for conforming and non-conforming contacts are different. Through calculation, we know that conforming contact has a linear relationship between total load and indentation depth, while that of non-conforming contact is nonlinear.

When an elastic layer is put into a solid, it will affect the distribution of the contact pressure in different levels depending on geometrical and physical parameters of both the layer and the solid. For instances, putting into softer middle layers will effectively decrease the contact pressure at the middle point of the contact area. For the ratio about 0.05 between thickness of the middle layer and the total thickness of the solid, change of middle layer Poisson's ratio has very little effect on the distribution of the contact pressure. While change of middle layer Young's modulus has influence on the contact pressure distribution, but not much. The results about their effects are demonstrated graphically and numerical solutions for contact pressures at different points in the contact area are also given for practical cases and further study. Finally the relationships between total loads and half contact lengths, total loads and indentation depths, half contact

lengths and indentation depths, are investigated and plotted in graphs for the guidance in the design and analysis of such layered structures under localized loadings.

4. 2 Future Work

In the present analysis, rigid punches are applied to solve the contact problems. This assumption is applicable for the cases that indenters are much stiffer than the elastic solid. Practically, we might meet similar indenters and solids. For this case, indenters cannot be treated as rigid punches. Therefore the displacement expression derived in the paper should be corrected for the deflection of the indenting surface. Some modification terms should be added. Another assumption in the study is frictionless, which is not so practical in reality. More work need to be done to consider the effect of the friction between the indenters and the solids.

BIBLIOGRAPHY

1. H. Hertz, *J. f. Math (crelle)*, Vol. 92 (1882), 156-171; *Miscellaneous papers [microform] / by Heinrich Hertz ... with an introduction by Philipp Leonard; authorised English translation by D.E. Jones ... and G.A. Schott ...*
2. A. E. H. Love, *A Treatise on the Mathematical Theory of Elasticity*, Cambridge, 1927.
3. C. Johnson, "An Elasto-plastic Contact Problem", *RAIRO Numer. Anal.*, 12 (1978), 59-74.
4. L. A. Galin, *Contact Problems in the Theory of Elasticity*, Gostekhizdat, 1953.
5. N. I. Muskhelishvili, *Some Basic Problems in the Mathematical Theory of Elasticity*, 3rd ed., Moscow, 1949, English Translation by J. R. M. Radok, Noordhoff, Leyden, the Netherlands, 1953.
6. A. I. Lure, *Three-Dimensional Problems of the Theory of Elasticity*, Interscience, New York, 1964.
7. G. M. L. Gladwell, *Contact Problems in the Classical Theory of Elasticity*, Sijthoff & Noordhoff, Alphen aan den Rijn, 1980.
8. I. N. Sneddon, *Fourier Transforms*, McGraw-Hill, New York, 1951.
9. M. Hannah, "Contact Stress and Deformation in a Thin Elastic Layer", *Quarterly Journal of Mech. And Appl. Math.*, Vol. IV, 1951, 94-105.
10. V. M. Aleksandrov, "On the Approximate Solution of a Certain Type of Integral Equation", *Prikl. Mat. Mekh.*, Vol. 26, 1962, 1410-1424.
11. V. M. Aleksandrov, "Some Contact Problems for the Elastic layer", *Prikl. Mat. Mekh.*, Vol. 27, 1963, 1164-1174.

12. V. M. Aleksandrov, "Asymptotic Methods in Contact Problems of Elasticity Theory", *Prikl. Mat. Mekh.*, Vol. 32, 1968, 691-703.
13. V. M. Aleksandrov, "Asymptotic Solution of the Contact Problem for a Thin Elastic Layer", *Prikl. Mat. Mekh.*, Vol. 33, 1969, 49-63.
14. R. D. W. Miller, "Some Effects of Compressibility on the indentation of a Thin Elastic Layer by a Smooth Rigid Cylinder", *Appl. Sci. Res.*, Vol. 16, 1966, 405-424.
15. P. Meijers, "The Contact Problems of a Rigid Cylinder on an Elastic Layer", *Applied Science Research*, Vol. 18, 1968, 353-383.
16. Y. Tu, "A numerical Solution for an Axially Symmetric Contact Problem", *Journal of Applied Mechanics*, Vol. 35, *Trans. ASME*, Vol. 89, Series F, No. 2, June 1967, 283-286.
17. T. S. Wu and Y. P. Chiu, "On the Contact Problem of Layered Elastic Solids", *Quart. Appl. Math.*, Vol. XXV, 1967, 233-242.
18. Y. C. Pao, T. S. Wu and Y. P. Chiu, "Bounds on the Maximum Contact Stress of an Indented Elastic Layer", *Journal of Applied Mechanics*, Vol. 38, *Trans. ASME*, Vol. 93, Series E, No. 3, Sept. 1971, 608-614.
19. J. B. Alblas and M. Kuipers, "On the Two Dimensional Problem of a Cylindrical Stamp Pressed into a Thin Elastic Layer", *Acta Mechanica*, Vol. 9, 1970, 292-311.
20. J. B. Alblas and M. Kuipers, "Contact Problems of a Rectangular Block on an Elastic Layer of Finite Thickness Part I: The Thin Layer", *Acta Mechanica*, Vol. 8, 1969, 133-145.
21. J. B. Alblas and M. Kuipers, "Contact Problems of a Rectangular Block on an Elastic Layer of Finite Thickness Part II: The Thick Layer", *Acta Mechanica*, Vol. 9, 1970, 1-12.
22. G. M. L. Gladwell, "On Some unbonded Contact Problems in Plane Elasticity Theory", *Journal of Applied Mechanics*, *Trans. ASME*, June 1976, 263-267.

23. A. Scalia and M. A. Sumbatyan, "Contact Problem for Porous Elastic Half-Plane", *Journal of Elasticity*, Vol. 60, 2000, 91-102.
24. A. Scalia, "Contact Problem for Porous Elastic Strip", *International Journal of Engineering Science*, Vol. 40, 2002, 401-410.
25. M. Wozniak, A. Hummel, and V. J. Pauk, "Axisymmetric Contact Problems for an Elastic layer Resting on a Rigid Base with a Winkler Type Excavitation", *International Journal of Solids and Structures*, Vol. 39, 2002, 4117-4131.
26. S. Timoshenko and J. N. Goodier, *Theory of Elasticity*, McGraw-Hill, New York, 1970.
27. Stephen Wolfram, *The Mathematica Book*, Wolfram Research Inc., 2001.
28. C. Lipson and R. C. Juvinall, *Handbook of Stress and Strength-Design and Material Application*, The Macmillan Company, New York, 1963.

MICHIGAN STATE UNIVERSITY LIBRARIES



3 1293 02328 7919